AUSTRIAN
MARSHALL PLAN FOUNDATION
VIENNA | AUSTRIA

UNI GRAZ

MARSHALL PLAN SCHOLARSHIP
FINAL RESEARCH REPORT = RESEARCH PAPER
COVER SHEET

Please complete this cover sheet on the computer, add the research paper resulting from the research stay undertaken at the University of Graz and send it in word-format and PDF-format to christa.grassauer@uni-graz.at.

PERSONAL DETAILS

First name	Petra	**Middle name**	
Last name	Frager		
Research period at host university (min = 3 full months excl. arrival and departure day)			
From (DD.MM.YY)	01.07.2016	**To (DD.MM.YY)**	21.12.2016

FINAL RESEARCH REPORT = Research Paper (min 7. 500 words excl. title page, table of content and references)

On the following pages provide the research paper resulting from the research stay undertaken at the host university.

Date (DD.MM.YYYY)	30.03.2017	**Signature**	Petra Frager

Petra Frager, BSc

The impact of the novel transcription factor CREBRF on adipocyte function

Final Report

Supervisor
Mag. Dr.rer.nat. Gabriele Schoiswohl
Institute of Molecular Biosciences
Karl-Franzens-University Graz

2016

Abstract

The number of people suffering from overweight and obesity has been significantly increasing in recent years. Overweight and obesity are considered as abnormal fat accumulations in multiple tissues, which are known to be risk factors for several health problems such as the coronary heart disease and diabetes mellitus and are therefore major contributors to morbidity and mortality.

Despite the alarming prevalence of obesity, causative genes and underlying mechanisms remain largely unexplained. Recently, the transcription factor CREBRF (Creb3 regulatory factor) has been implicated in the regulation of lipid and energy metabolism. A genome-wide association study identified a missense variant in the transcriptional regulator CREBRF that increases obesity risk, but provides relative protection from obesity-related metabolic complications. Moreover, studies in murine adipocytes demonstrated that overexpression of CREBRF and its obesity-risk variant improves adipogenesis, promotes lipid accumulation, and modulates mitochondrial function in murine adipocytes. The aim of this study is to evaluate the regulation of Crebrf expression in adipocytes and to determine the contribution of overexpressing CREBRF and its obesity-risk variant to adipocyte function.

Crebrf expression is regulated by nutritional status such as fasting. Its expression increases during adipogenesis in murine and human adipocytes. Interestingly, deletion of Crebrf in mice increases total body fat mass, but has no influence on the expression of adipogenic markers in different adipose tissue deposits, suggesting that CREBRF modulates lipid storage but has no direct effect on adipogenesis. To investigate the effect of overexpressing CREBRF and its mutant in human adipocytes we generated stably overexpressing cells using lentiviruses. Preliminary data demonstrate that overexpressing CREBRF and its obesity-risk variant increased mitochondrial respiration in preadipocytes, suggesting that CREBRF directly affects mitochondrial function.

Content

1. Introduction

The number of people suffering from overweight and obesity has been significantly increasing increased in recent years. According to the World Health Organization the number of obese people has more than doubled since 1980 [1]. This rise of overweight people among the global population is driven by several reasons like genetic disposition, the abundance of high-energy containing food, and diminished physical activity in modern civilization. Overweight and obesity are considered as abnormal fat accumulations, which are known to be risk factors for several health problems like the coronary heart disease and diabetes mellitus and are therefore major contributors to morbidity and mortality [2].

1.1 Adipose Tissue

Excess energy that is consumed and not spent is mostly stored in form of triglycerides in adipocytes within the adipose tissue. Although adipocytes are the most abundant cells of the adipose tissue, it is still very heterogeneous and contains many cell types including precursor cells (preadipocytes), fibroblasts, endothelial cells, vascular smooth muscle cells, and immune cells [3]. There are two types of adipose tissue, the white adipocyte tissue (WAT) and the brown adipose tissue (BAT). They are distinguished because of their different morphology and cellular properties [4].

1.1.1 White adipose tissue (WAT)

The visceral fat pads (intraabdominal) and the subcutaneous fat pads (hypodermis) are the two major WAT depots. Adipocytes of the WAT only contain a single lipid droplet in the cytoplasm which almost accounts for the entire cell volume [5]. A dense network of vascular cells in the WAT provides for substrates and oxygen and facilitates access to signaling molecules [6]. In addition to its function in energy storage, the WAT is also involved in metabolic homeostasis by secreting hormones and adipokines [5]. Obesity can cause an imbalance in the release of pro- and anti-inflammatory cytokines resulting in chronic inflammation that is linked to insulin resistance, type two diabetes mellitus, hypertension, and cardiovascular disease [7]. While visceral adipocytes produce more pro-inflammatory cytokines like IL-6, subcutaneous adipocytes mainly secrete leptin and adiponectin [5].

1.1.2 Brown adipose tissue (BAT)

The biggest BAT depot in mice, which is characterized by its brown appearance, is found in the intrascapular and dorso-cervical region. The color is a result of the high amount of iron and cytochrome and by the high density of the vascular network. The primary function of the BAT is heat production through metabolization of energy substrates. Brown adipocytes of the BAT contain several lipid droplets and have a high quantity of mitochondria, this provides for the high capacity for substrate oxidation in

order to produce heat [8]. The existence of active BAT in humans has only been recognized in 2007. Active BAT is not present in every human and the amount declines correlating with age and obesity [9].

1.2 Adipogenesis

Although the number of adipocytes in human adults is steady, about 10% of fat cells are regenerated each year [10]. This turnover rate is even higher for murine adipose tissue, where 1-5% of adipocytes are renewed daily [11]. Adipocytes derive from mesenchymal stem cells (MSCs). The development from MSCs to adipocytes is called adipogenesis and is separated into two phases: commitment and terminal differentiation [12]. Figure 1-1 shows a model of adipogenesis of mesenchymal stem cells into white adipocytes.

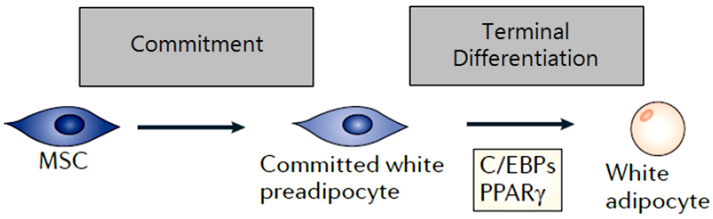

Figure 1-1: Model of adipogenesis. Mesenchymal stem cells (MSCs) turn into committed white preadipocytes during the commitment phase of adipogenesis. The second phase called terminal differentiation is tightly regulated by the transcription factors (C/EBPs and PPARγ) [13].

The commitment phase of MSCs is very complex and not yet fully understood. This process is dependent of many different influences like TGFβ superfamily signaling, RHO-associated kinase (ROCK) signaling, the structure of the extra cellular matrix (ECM), cell-cell contacts and the cell shapes.

Committed white preadipocyte do not spontaneously enter terminal differentiation. They have to be stimulated by effectors like glucocorticoids, insulin and cyclic AMP [13]. Stimulated preadipocytes undergo four steps including growth arrest, mitotic clonal expansion, early and terminal differentiation that are very tightly regulated by a complex gene expression pattern [14].

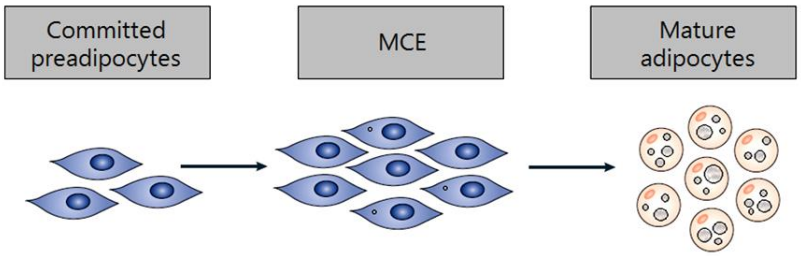

Figure 1-2: Model of terminal differentiation. Committed preadipocytes re-entry cell cycle for mitotic clonal expansion (MCE). This process is tightly regulated by transcription factors. Cell morphology is changing drastically during terminal differentiation caused by lipid accumulation [14].

Figure 1-2 shows the process of terminal differentiation of committed preadipocytes to mature adipocytes filled with lipid droplets. In course of differentiation, preadipocytes re-entry the cell cycle for about two rounds of mitosis, which is called mitotic clonal expansion (MCE) [15]. In early differentiation

there is an increase of cyclic adenosine monophosphate (cAMP) levels stimulating protein kinase A (PKA). PKA activates the cyclic-AMP-responsive element binding (CREB) protein. This transcription factor promotes the expression of pro-adipogenic transcription factors like the CCAAT-enhancer-binding proteins (*C/EBPs*) and proliferator activated receptor γ (*PPARγ*) [16]. *C/EBPα* and *PPARγ* have antimitotic properties and appear to be terminators of the MCE [15]. Full differentiation into mature adipocytes further requires other factors like Krupel-like factors (*KLFs*) Wingless and INT-1 proteins (*Wnts*) and cell-cycle proteins, which interact at different stages during adipogenesis [17].

1.3 Lipid metabolism

Adipose tissue serves as an energy storage organ. Spare energy is stored effectively in form of triglycerides (TG) in lipid droplets. In the fed state when energy is abundant, the biosynthesis of TGs via the lipogenic pathway increases the size of lipid droplets. Upon starvation, the lipolytic pathway is activated and TGs are hydrolysed into free fatty acids (FFAs) and glycerol, which are either subject to further oxidation or are released from the cell. In figure 1-3, both pathways are depicted in a model [18].

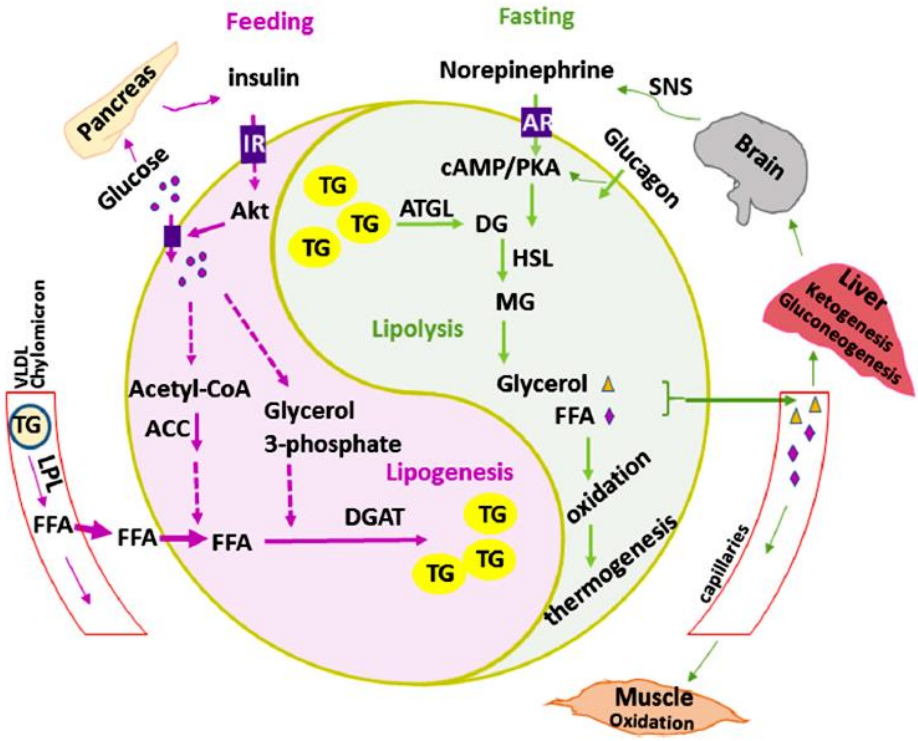

Figure 1-3: Model of the lipid metabolism of adipocytes. Adipocytes are able to respond to nutrient availability by entering the lipolytic or lipogenic pathway in order to maintain energy homeostasis. These pathways are sensitive to nutrients like glucose and free fatty acids (FFAs) as well as hormones like insulin, norepinephrine due to receptors on the cell surface (IR, insulin receptor; AR, adrenergic receptor). Fasted cells promote lipolysis to hydrolyze TG into FFAs and glycerol, which are subsequently oxidized or released. They enter the bloodstream and are transported to the liver, muscle, and other organs. Fed cells enter the lipogenic pathway, where fatty acids are generated from glucose and are further used for biosynthesis of TGs [18].

1.4 The human transcription factor *CREBRF*

CREB3 (Cyclic-AMP-responsive element binding) is a transmembrane protein located at the endoplasmic reticulum (ER). It's the most abundant member of the Cyclic-AMP-responsive element binding protein family. These proteins are known to be mammalian transcription activators [19]. Upon accumulation of unfolded proteins at the ER, *CREB3* is subject to proteolytic cleavage and gets released [20]. Subsequently *CREB3* activates downstream stress response-related genes. They contribute to restore homeostasis in the ER which is crucial for cell survival [21,22].

CREBRF (Creb3 regulatory factor) is a protein that acts as a negative regulator of *CREB3*. It is able to recruit and promote degradation of nuclear *CREB3*. *CREBRF* proofed to be highly unstable with a half-life of ~20 min, due to proteosomal degradation. Half-life of *CREBRF* can be improved by the proteosomal inhibitor MG132 [23].

1.5 The natural occurring variant of human *CREBRF (R457Q)*

A genome-wide association study performed in 3,072 Samoan individuals, a Polynesian ethnic group with a high prevalence of obesity, identified a naturally occurring missense variant of *CREBRF (R457Q)*. This variant encodes for a protein where the arginine-residue (R) on position 457 is replaced by a glutamine-residue (Q). Results of this study indicated that the *R457Q* allele increases obesity risk but provides relative protection from obesity-related metabolic complications. Moreover, studies in murine adipocytes demonstrated that overexpression of CREBRF and its obesity-risk variant improves adipogenesis, promotes lipid accumulation, and modulates mitochondrial function in murine adipocytes [24].

1.6 Aim of the study

Despite the alarming prevalence of obesity, causative genes and underlying mechanisms remain largely unexplained. Preliminary data suggest that mammalian CREBRF plays a key role in adipocyte biology, cellular lipid homeostasis and energy substrate utilization. Our hypothesis is that changes of the transcriptional response mediated by CREBRF will alter human adipocyte function by modulating lipid metabolism (lipid synthesis, lipid storage, and/or mobilization) and or by modulating energy homeostasis (energy substrate uptake and utilization). The central aim of this study is to determine the regulation of CREBRF in murine and human adipocytes as well as to determine the contribution of overexpressing CREBRF and its obesity-risk variant to adipocyte function.

2. Methods

2.1 Cell Culture

Cells were generally cultured in a humidified atmosphere supplemented with 5% CO_2 at 37°C and passaged before reaching confluence.

2.1.1 Differentiation of 3T3-L1 cells

The murine preadipocyte cell line was cultured as described before [1]. Briefly, 3T3-L1 cells were cultured in DMEM High glucose with 4,500 mg/L glucose, sodium pyruvate, sodium bicarbonate and 25 mM HEPES supplemented with 10% fetal bovine serum and 100µg/mL penicillin and streptomycin. Cells were seeded in Greiner Bio One CELLSTAR® 6 well culture plates at a density of 2.5 x 10^5 cells/well. Two days after cells reached confluence, differentiation was induced by changing to DMEM Differentiation Media I, containing 1 µg/mL Insulin solution from bovine pancreas, 0.25 µM Dexamethasone, 500 µM Methylisobuthylxantine and 2 µM Rosiglitazone. After 48h media was changed to DMEM Differentiation Media II containing 1 µg/mL Insulin. After another 48h, media was changed back to DMEM High Glucose media, and was refreshed every 48h.

2.1.2 Inducing nutritional stress in 3T3-L1 cells

3T3-L1 preadipocytes (two days after reaching confluence) and 3T3-L1 adipocytes (14 days after inducing differentiation) were put under nutritional stress. To induce this condition cells were treated with Hank's Balanced Salt Solution (HBSS), serum-free DMEM containing 2% BSA (FA-free) or DMEM containing 20 ng/mL Rapamycin. Cells were treated for 2h, 4h, 6h, 12h, and 24h or were treated for 12h and then re-fed normal DMEM High Glucose media for another 12h.

2.1.3 Differentiation of Human Pre-Adipocyte Cells (HPACs)

Human Adipocyte Precursor Cells (HPACs) were cultured in basal StemLife™ MSC Medium containing L-Alanyl-L-Glutamine Life Factor and MSC Life Factor. HPACs were seeded in Falcon™ Tissue Culture 12 well plates at a density of 18,000 cells/cm^2. After 72h adipogenesis was induced by changing to AdipoLife Adipogenesis Initiation Medium. After 48h each well was re-fed 0.5mL AdipoLife Adipogenesis Initiation Medium. After another 48h each well was re-fed with 1mL of AdipoLife Adipogenesis Maintenance Medium every 3-4 days.

2.1.4 Differentiation of Simpson-Golabi-Behmel Syndrome (SGBS) cells

SGBS cells were cultivated according to standard protocols [25]. Briefly, cells were cultured in SGBS Growth media, DMEM / F12 (1:1) with L-Glutamine and 15 mM HEPES supplemented with 8 µg/mL Biotin, 4 µg/mL D-Pantothenic acid, 10% fetal bovine serum and 100 µg/mL penicillin and streptomycin.

Cells were seeded at a density of 11,000 cells/well in Falcon™ Tissue Culture 12 well plates. Differentiation was started when cells were almost confluent by changing to serum-free SGBS Differentiation Media I, containing 0.01 mg/mL apo-Transferrin human, 0.1 µM Hydrocortisone 21-hemisuccinate sodium salt, 200 pM Triodotyronine, 20 nM human Insulin, 0.25 µM Dexamethasone, 500 µM Methylisobuthylxantine and 2 µM Rosiglitazone. On day 4 media was changed to SGBS Differentiation Media II, where Rosiglitazone was omitted. On day 7 and 11 of differentiation, media was changed to SGBS Differentiation Media III (Dexamethasone and Methylisobuthylxantine were omitted). On day 14 cells were fully differentiated into adipocytes and media was changed to Insulin-free DMEM / F12 (1:1) with L-Glutamine and 15 mM HEPES.

2.1.5 Measuring mitochondrial function of SGBS pre- and adipocytes

SGBS cells were seeded at a density of 1,000 cells in 180 µL per well in 96-well Seahorse XF96 Cell Culture Microplates (Agilent Technologies). SGBS cells were cultured as described above. Mitochondrial function has been measured of cells in the preadipocyte state and of cells on day 7 and 14 after induction of adipogenesis. Media was changed to unbuffered assay medium before measurement (DMEM with 4.5 g/L glucose) and cells were kept in a non-CO_2 incubator at 37°C until start of the assay.

2.1.6 Producing Lentiviral Supernatants using Human embryonic kidney (HEK-293T) cells

To produce Lentiviral Supernatants 4.5 x 10^6 HEK-293T cells were seeded in 100 mm culture dishes. Cells were cultured in tetracycline-free DMEM (High glucose with 4,500 mg/L glucose, sodium pyruvate, sodium bicarbonate and 25 mM HEPES supplemented with 10% tetracycline-free fetal bovine serum and 100 µg/mL penicillin and streptomycin.

Plasmid-DNA of the pLVX-Tight-Puro Vector containing an eGFP, human *CREBRF-WT* or human *CREBRF-RQ* insert and the pLVX-Tet-Off Advanced Vector plasmid-DNA was mixed with Lenti-X™ Packaging Single Shots according to manufacturer's instructions and added to HEK-293T cells. The lentivirus containing supernatants were collected after 48h, and were centrifuged at 1000 rpm before transduction.

2.1.7 Generation of stable SGBS preadipocyte cell lines

SGBS preadipocytes have been seeded in 6-well plates at a density of 20,000 cells/well in tetracycline-free SGBS Growth Media. After 24h, 4 µg/mL Polybrene (Hexadimethrine bromide, Sigma-Aldrich, Inc.) has been added to the media to optimize transduction efficiency. Co-Transduction has been performed by adding 100 µL lentiviral supernatant of LVX-Tet-Off Advanced and LVX-Tight-Puro with the respective insert (eGFP, human *CREBRF-WT* or human *CREBRF-RQ*) to each well. Media was changed after 24h and cells have been subjected to selection using 500 µg/mL Puromycin (Sigma-Aldrich, Inc.) for three weeks to generate stable cell lines.

2.1.8 Measuring mitochondrial function of SGBS preadipocytes overexpressing human *CREBRF-WT* or *CREBRF-RQ*

Stable overexpressing SGBS preadipocytes were seeded at a density of 1,000 cells in 180µL per well in 96-well Seahorse XF96 Cell Culture Microplates (Agilent Technologies) in tetracycline-free SGBS Growth Media. Preadipocytes were cultured for one week and media was changed every second day. Media was changed to unbuffered assay medium before measurement (DMEM with 4.5 g/L glucose) and cells were kept in a non-CO_2 incubator at 37°C until start of the assay.

2.2 Oil Red O Staining

3T3-L1 cells, HPACs, and SGBS cells have been stained with the Oil Red O Staining Kit (Lifeline Cell Technology) on several time points during adipogenesis. The Fixation and Staining were performed according to the supplier's manual. In short, cells were washed three times with 1xPBS and fixed for 20 min at RT using 4% Paraformaldehyde Fixative Solution. Each well was rinsed twice with deionized water, and cells were treated twice with 100% 1,2-Propanediol Dehydration Solution for 5 min. Oil Red O Stain Solution was added to each well and the plates were incubated at 37°C for 30min. Then, the cells were counter stained by adding 85% 1,2-Propanediol Stain Differential Solution for 1 min. Cells were washed twice and kept in deionized water at 4°C until microscopy.

2.2.1 Microscopy of Oil Red O stained cells

Oil Red O stained cells have been visualized using a Nikon Eclipse TS100 inverted microscope with a 20x Plan Fluor objective. The Images have been digitalized using the SPOT 5.1 Advanced software.

2.2.2 Oil Red O extraction and quantification of lipid accumulation

After microscopy, deionized water was removed and cells were allowed to dry for 24h. Oil Red O was extracted from cells by adding 300 µL Isopropanol to each well and incubating the plates at RT and 80 rpm for 1h. Optical density of the extraction was measured using the Multiskan™ GO Microplate Spectrophotometer at a wavelength of 512 nm, Isopropanol was used as a blank.

After extraction, 3T3-L1 and HPAC cells were left to dry for 3h, and 500 µL Lysis-Buffer I was added to each well. After 24h of incubation at RT and 80 rpm, protein-content was measured using Pierce-BCA Kit.

After extraction of Oil Red O from SGBS cells, 500 µL Lysis-Buffer II was added to each well of dried cells and plates were incubated for 24h. After this, plates were sonicated for 5 min at Amplitude 2. Protein-content was measured using Pierce-BCA Kit and was used for normalization of Optical Density (OD_{512}).

2.3 Seahorse XF Cell Mito Stress Test

The Seahorse XF Cell Mito Stress Test was performed as recommended by the manufacturer. Plates containing 180 µL unbuffered media (DMEM with 4.5 g/L glucose) per well were placed on the instrument tray of the analyzer. In course of the assay, modulators of cellular respiration have been added successively to each well at the designated time points and concentrations shown in figure 3-18a and 3-20a.

By directly measuring the oxygen consumption rate (OCR) of the cells during the assay, it is possible to determine parameters like ATP production, basal and maximal respiration, non-mitochondrial respiration, and basal glycolysis. After the assay was finished, cells were lysed using Lysis-Buffer I and protein concentration was determined (Pierce-BCA Kit) to normalize data.

2.4 Animals

All animal procedures were evaluated and approved by the University of Pittsburgh's Institutional Animal Care and Use Committee. Mice were housed at 25°C under 14h-light/10h-dark cycles and provided with food and water available *ad libitum*. The Prolab®Isopro®RMH 3000 Chow Diet was purchased from LabDiet® (St. Louis, USA) and contained 26.0 kcal% protein, 59.7 kcal% carbohydrate and 14.3 kcal% fat. High Fat Diet (HFD) was purchased from Research Diets, Inc. and contained 20 kcal% protein, 35 kcal% carbohydrate and 45 kcal% fat.

2.4.1 Collecting samples of mice on Chow or High Fat Diet (HFD)

12 week old C57/BL6-N mice were fed Chow or High Fat Diet (HFD) for eight weeks and fasted for 4h before adipose tissue (BAT, brown; PGAT, perigonadal; and SCAT subcutaneous adipose tissue) was collected and homogenized in 1 mL TRIzol® Reagent (life technologies™) per 100 mg tissue.

2.4.2 Collecting samples of Crebrf-WT and Crebrf-KO mice

Crebrf-KO C57/BL6-J mice strain was generated and kindly provided by Ray Lu (Department of Molecular and Cellular Biology, University of Guelph, Guelph, Ontario, Canada) [26]. 21 week old C57/BL6-J Crebrf-WT and Crebrf-KO mice fed Chow Diet were fasted for 16h before adipose tissue was collected and homogenized as described above.

2.5 RNA extraction and quantitative RT-PCR

Cells for RNA isolation were lysed using 100 µL TRIzol®Reagent per 1 cm^2 culture dish surface area. RNA of lysed cells and homogenized tissue was extracted according to the manufacturer's instructions. To remove residual genomic DNA, samples were treated with DNaseI, Amplification Grade (Invitrogen™) as recommended by the manual. One µg RNA of each sample was used for cDNA synthesis using qScript

cDNA SuperMix (Quanta Biosciences). Samples were diluted and 1 ng cDNA was used as a template for quantitative RT-PCR. Relative mRNA concentration of murine samples was determined in comparison to a pooled standard made from cDNA samples isolated from perigonadal adipose tissue of different mice which was serially diluted in the range from 50 ng - 0.05 pg. Relative mRNA concentration of human samples was determined in comparison to a pooled standard made from cDNA samples of differentiated HPACs, diluted in the same way.

Quantitative RT-PCR was performed using the Eppendorf Mastercycler® RealPlex^2. Templates were mixed with PerfeCTa SYBR® Green FastMix or PerfeCTa® FastMix® II (Quanta Biosciences) and respective primers listed in table 2-1 and 2-2. RT-PCR was performed according to the manufacturer's instructions. For each sample, the relative mRNA concentration of genes of interest was further normalized to the mRNA-amount of the housekeeping gene cyclophilin.

Table 2-1: List of Primer-sequences used for quantitative RT-PCR using PerfeCTa SYBR® Green FastMix

Species	Target	Type	Sequence
Mus musculus	Crebrf	forward	5'-GAGGACTTGAAGGAGATGACG-3'
		reverse	5'-CAGAAGGCCTCAGAATCCTC-3'
Mus musculus	Pparg1	forward	5'-AACAAGACTACCCTTTACTGAAATTACCA-3'
		reverse	5'-CACAGAGCTGATTCCGAAGTTG-3'
Mus musculus	Pparg2	forward	5'-CCAGAGCATGGTGCCTTCGCT-3'
		reverse	5'-CAGCAACCATTGGGTCAG-3'
Homo sapiens	CYCLOPHILIN	forward	5'-ATGTGTCAGGGTGGTGACTTC-3'
		reverse	5'-GCCATCCAACCACTCAGTCTT-3'
Homo sapiens	CEBPB	forward	5'-GATGTTCCTACGGGCTTGTTG-3'
		reverse	5'-CCCCAAAAGGCTTTGTAACCA-3'
Homo sapiens	PPARG2	forward	5'-CTGCAGGTGATCAAGAAGACG-3'
		reverse	5'-GGAAGAAGGGAAATGTTGGCA-3'

Table 2-2: List of Primer-sequences, TaqMan Probes and TaqMan® Assays used for quantitative RT-PCR using PerfeCTa® FastMix® II

Species	Target	Type	Sequence	Origin
Mus musculus	Cyclophilin	forward	5'-GGTGGAGAGCACCAAGACAGA-3'	LGC Biosearch Technologies
		reverse	5'-GCCGGAGTCGACAATGATG-3'	LGC Biosearch Technologies
		TaqMan Probe	(HEX)-5'-AGCCGGGACAAGCCACTGAAGGAT-3'-(BHQ1)	LGC Biosearch Technologies
Mus musculus	Cebpa	TaqMan® Assay	Mm00514283	applied biosystems™
Mus musculus	Adiponectin	TaqMan® Assay	Mm00456425	applied biosystems™
Mus musculus	Fasn	TaqMan® Assay	Mm00662319	applied biosystems™
Mus musculus	Dgat2	TaqMan® Assay	Mm01273905	applied biosystems™
Homo sapiens	CREBRF	TaqMan® Assay	Hs01078210_m1	applied biosystems™
Homo sapiens	CEBPA	TaqMan® Assay	Hs00269972_s1	applied biosystems™

2.6 Cloning

In order to generate Lentiviruses overexpressing genes of interest, they have to be cloned into the multiple cloning site of the plasmid. Therefore CREBRF-WT, CREBRF-RQ and eGFP sequences had to be inserted into the pLVX-Tight-Puro-Vector.

2.6.1 Amplification of GFP, hCrebrf-WT and hCrebrf-RQ sequences using PCR

GFP, hCrebrf-WT and hCrebrf-RQ sequences were amplified using PCR with TaKaRa LA Taq® DNA polymerase and buffer purchased from Takara Bio USA, Inc. Primers used for the reactions are shown in table 2-3 and were purchased from Integrated DNA Technologies, Inc.

Table 2-3: List of Primer-sequences used for cloning purposes

Product	Type	Sequence	Tm [°C]
GFP	forward	5'-TAATATACGCGTGCCACCATGGTGAGCAAGGGCGAGGA-3'	73.3
	reverse	5'-TTCACGCGTCTAGTGATGGTGATGGTGATGCAGAT-3'	69.2
human CREBRF-WT	forward	5'-CCGCTCGAGATGCCTCAGCCTAGTGTAAGC-3'	69.7
	reverse	5'-CCGCTCGAGCACCTTTGATGTTGGTATCCT-3'	67.4
human CREBRF-RQ	forward	5'-TAATATACGCGTGCCACCATGCCTCAGCCTAGTGTAAG-3'	69.0
	reverse	5'-TTCACGCGTCTAGTGATGGTGATGGTGATGCAGAT-3'	69.2

Primers used for amplification also introduced binding sites for restriction enzymes into the sequence. Amplification was performed with temperatures according to the program shown in table 2-4.

Table 2-4: Program for PCR-reactions using the T100™ Thermal Cycler (BIO-RAD)

Step	Temperature [C°]	Time	
Initial Denaturation	95	3 min	
Denaturation	95	30 sec	}35x
Primer Annealing	62	30 sec	
Elongation	72	2 min	
Final Elongation	72	5 min	
Hold	4	∞	

2.6.2 DNA agarose gel electrophoresis

To control the size of the amplicons, PCR-reactions were size separated using agarose gel electrophoresis. DNA was separated using a 1% agarose gel. The DNA Standard Lambda DNA/HindIII Marker (Thermo Scientific™) was used to infer sizes of the amplicons. Gels were run at 100V for 60 min in 1xTAE Buffer (national diagnostics).

2.6.3 DNA-Elution

DNA-Fragments were cut out from the agarose gel and DNA was eluted using the High Pure PCR Product Purification Kit (Roche Molecular Systems Inc.).

2.6.4 TA-Cloning

Crebrf-RQ and eGFP PCR-Reactions were used for direct cloning into the pCR™ 2.1-TOPO® TA Vector (life technologies™) according to the manufacturer's instructions.

2.6.5 Digestion of DNA with restriction enzymes

Crebrf-RQ- and eGFP-Inserts were cut out of the pCR™ 2.1-TOPO® TA Vector using the restriction enzymes EcoRI and MluI in NEBuffer 3.1 (New England Biolabs) at 37°C for 2h. The receiving pLVX-Tight-Puro Vector was also cut with the same enzymes to ensure incorporation of the insert in the correct orientation.

For cloning of the Crebrf-WT-Insert into the pLVX-Tight-Puro Vector, the vector was first cut with the restriction enzyme NotI in NEBuffer 3.1 (New England Biolabs) at 37°C for 2h. The linearized vector was blunted using TaKaRa LA Taq® DNA polymerase and buffer (Takara Bio USA, Inc.) for 2 min at 95°C, followed by 15 min at 72°C using the T100™ Thermal Cycler (BIO-RAD). The blunted vector was cut again in a second restriction using the enzyme MluI in NEBuffer 3.1 (New England Biolabs) at 37°C for 2h. The Crebrf-WT Fragments were also cut with the restriction enzyme MluI in the same manner.

2.6.6 Ligation and transformation of DNA constructs into *E. coli* C2984I

Ligation was performed using a 1:5 vector-insert ratio considering DNA-fragment size (bp). T4 DNA Ligase and buffer were purchased from New England Biolabs. The reaction was incubated at RT for 2h before transformation.

NEB® Turbo Competent *E. coli* (High Efficiency) C2984I cells were used as chemically competent cells for cloning of gene constructs using heat shock transformation. Cells were thawed, mixed with ligation reaction and incubated on ice for 20 min. Heat shock was performed for 30 sec at 42°C. After adding SOC-medium (New England Biolabs), the transformation reaction was incubated for 1h at 37°C at 200 rpm before spreading on selective LB Agar plates (Molecular Biology Certified™) containing 1µL/mL Ampicillin (Sigma-Aldrich, Inc.).

2.6.7 Plasmid isolation

LB Medium (MP Biomedicals) supplemented with 1µL/mL Ampicillin (Sigma-Aldrich, Inc.) was inoculated with colonies of positive clones and were incubated at 37°C at 200rpm overnight. Plasmid DNA was isolated using the HiSpeed Plasmid Midi Kit (QIAGEN N. V.) according to the manufacturer's instructions. Plasmid-DNA was sent for sequencing to verify insertion of the gene of interest.

2.7 Statistical methods

Data are generally shown as the mean ± standard error of the mean (SEM). MS Excel was used to analyze statistical significance using a two-tailed *t*-test. Significance was considered at a p-value$\leq$0.05.

3. Results

3.1 Nutritional status regulates endogenous Crebrf expression in murine 3T3-L1 cells

Recently, Tiebe et al. showed that starvation induces the expression of the *CREBRF* orthololog "REPTOR" in *Drosophila melanogaster*. REPTOR is a downstream transcription factor of the Target of rapamycin complex 1 (TORC1), which regulates growth and metabolism. When cellular energy amount is low, reflected by low ATP- and high AMP-levels, mTORC1 is inactivated to conserve limited resources. Inhibition of mTORC1 that prevents anabolic downstream signaling can also be achieved by Rapamycin. Upon TORC1 inhibition by starvation or by rapamycin treatment, REPTOR is dephosphorylated, translocated to the nucleus and enabling transcription of target genes [27]. To evaluate whether murine Crebrf is also regulated by nutritional stress, we measured endogenous Crebrf expression in 3T3-L1 preadipocytes and adipocytes. Cells were either treated with Hank's Balanced Salt Solution (HBSS; with glucose, but no amino acids), serum-free DMEM containing 2% BSA (with glucose and amino acids, but no FA) or DMEM containing 20 ng/mL Rapamycin. Crebrf expression was measured by RT-qPCR on several time points. Starving and Rapamycin treatment of 3T3-L1 cells induced CREBRF expression in both preadipocytes and adipocytes (Figure 3-1 and 3-2). Re-feeding of starved cells abrogates this effect, and CREBRF expression is lower than at baseline. These results indicate that murine CREBRF is regulated by nutritional status and might act as a downstream transcription factor of the mechanistic Target of Rapamycin (mTOR), similar to the way shown in *Drosophila melanogaster*.

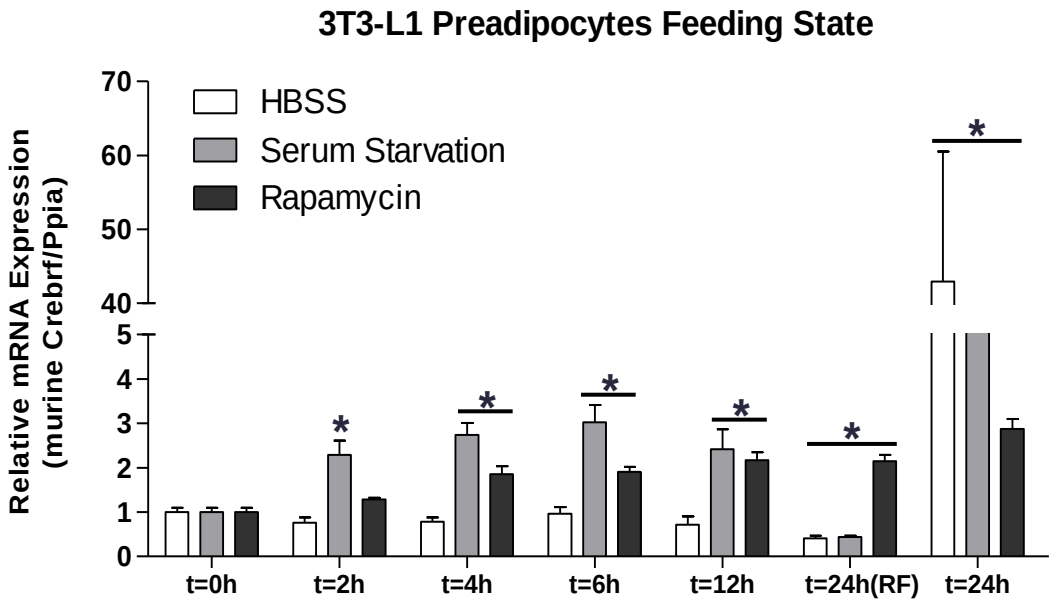

Figure 3-1: Endogenous mRNA expression of Crebrf in murine 3T3-L1 preadipocytes. Expression was measured using RT-qPCR on indicated time points after induction of nutritional stress (t=0h). The abbreviation RF indicates that cells were re-fed with complete medium after 12 h. Relative mRNA expression of Crebrf was normalized to the housekeeping gene Cyclophilin (peptidylprolyl isomerase A; PPia) with t=0h group arbitrarily set to 1 . $p \leq .05$: * effect of treatment.

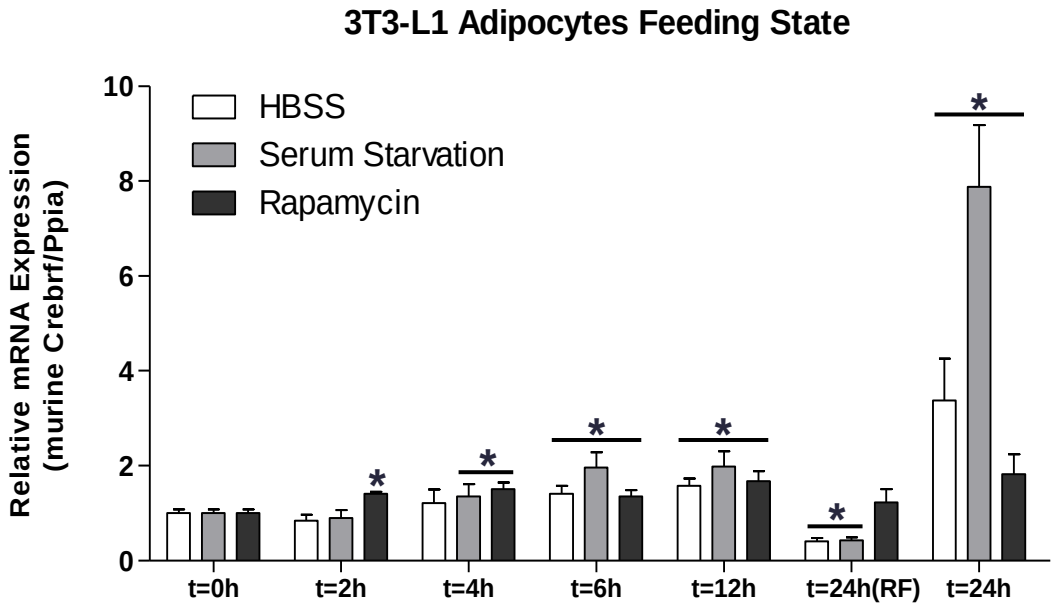

Figure 3-2: Endogenous mRNA expression of Crebrf in murine 3T3-L1 adipocytes. Expression was measured using RT-qPCR on indicated time points after induction of nutritional stress (t=0h). The abbreviation RF indicates that cells were re-fed with complete medium after 12 h. Relative mRNA expression of Crebrf normalized to the housekeeping gene Cyclophilin (peptidylprolyl isomerase A; PPia) in adipocytes (day 14 of differentiation) with t=0h group arbitrarily set to 1. $p \leq .05$: * effect of treatment.

Since murine Crebrf expression increases upon mTORC1 inhibition, we evaluated whether insulin which prevents mTORC1 inhibition [28] also affects Crebrf. 3T3-L1 adipocytes were treated with insulin and rapamycin to mimic high and low nutritional status in cells. Insulin treatment reduced Crebrf expression while rapamycin again increased its expression. Notably, cells treated with both, insulin and rapamycin, showed no changes in Crebrf expression. Overall, these data show that endogenous Crebrf expression is directly affected by mTORC1 activity (Figure 3-3).

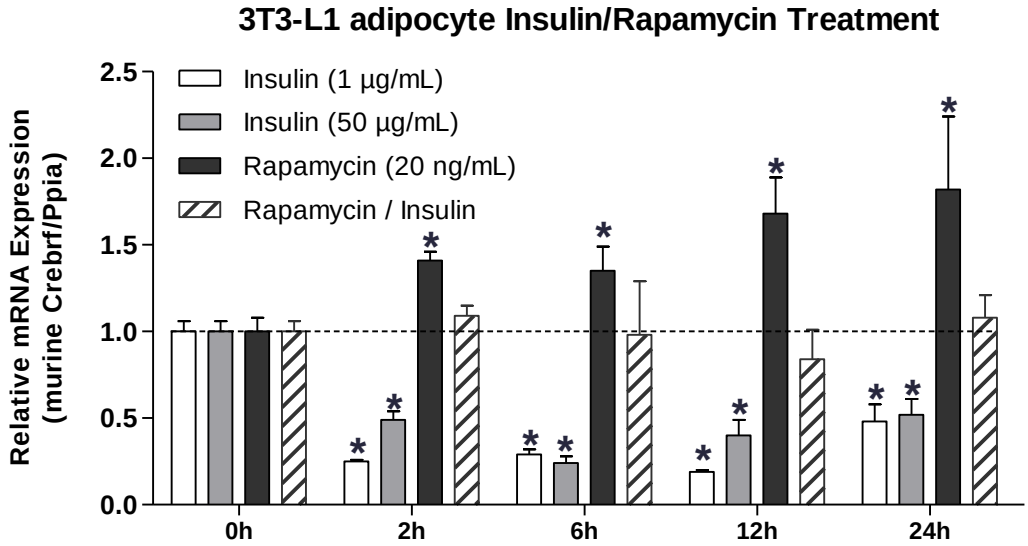

Figure 3-3: Endogenous expression of Crebrf in 3T3-L1 adipocytes in response to nutritional status. Relative expression of Crebrf in 3T3-L1 adipocytes is influenced by mimicking nutritional status by activating (with Insulin) or inhibiting (with Rapamycin) the mammalian Target of Rapamycin Complex 1 (mTORC1). Samples were generated on indicated time points and mRNA expression was measured using RT-qPCR. Relative mRNA expression of Crebrf is normalized to the housekeeping gene Cyclophilin (peptidylprolyl isomerase A; PPia). $p \leq .05$: * effect of treatment.

3.2 Crebrf expression in 3T3-L1 adipocytes is decreased by β-adrenergic agonists

Metabolic pathways are strongly influenced by cyclic AMP signaling. cAMP, which is known to play a significant role in adipogenesis, is also involved in lipid metabolism of the white adipose tissue. During fasting, cells try to achieve nutritional homeostasis by hydrolyzing stored triglycerides in a process called lipolysis. Catecholamines (i.e. Epinephrine and Norepinephrine) are the main triggers of lipolysis in humans by activating membrane-bound adrenergic receptors. cAMP production is stimulated by activation of β-adrenergic receptors (β1, β2, and β3). Increased levels of cAMP promote lipolytic pathways [16]. Treatment of 3T3-L1 adipocytes with the β-adrenergic agonists Isoproterenol (β1- and β2-receptor), Forskolin (β2-receptor), and CL (β3-receptor) was performed to see if endogenous Crebrf expression is influenced by elevated cAMP levels. Activation of β-adrenergic receptor decreased endogenous Crebrf expression (Figure 3-4), indicating that Crebrf expression is reduced under sufficient substrate availability such as lipids (fatty acids).

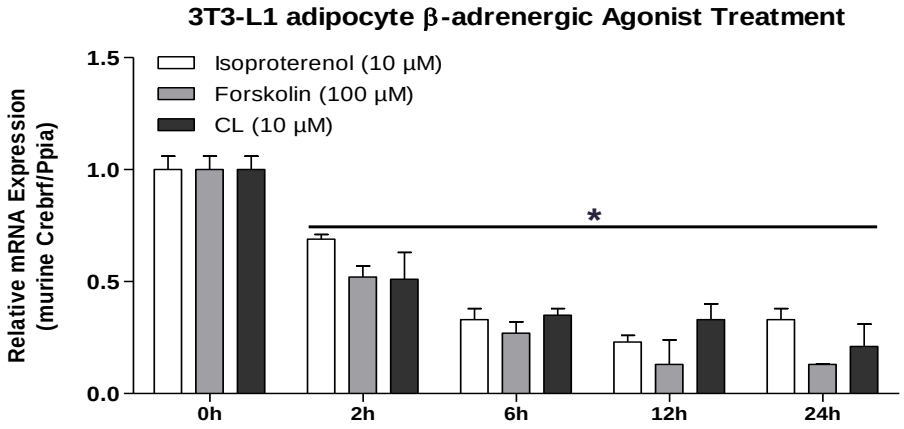

Figure 3-4: Endogenous expression of Crebrf in 3T3-L1 adipocytes in response to β-adrenergic receptor stimulation. Relative expression of Crebrf in 3T3-L1 adipocytes is decreased by β-adrenergic-agonists: Isoproterenol (β1- and β2-receptor), Forskolin (β2-receptor) and CL (β3-receptor). Samples were generated on indicated time points and mRNA expression was measured using RT-qPCR. Relative mRNA expression of Crebrf is normalized to the housekeeping gene Cyclophilin (peptidylprolyl isomerase A; PPia). $p \leq .05$: * effect of treatment.

3.3 Crebrf expression in mature 3T3-L1 adipocytes is not affected by differentiation stimulating hormones

Mature 3T3-adipocytes were treated with the components of the hormonal differentiation cocktail, including dexamethasone (glucocorticoid), Rosiglitazone (PPARγ agonist), and IBMX (inhibits cAMP-Phosphodiesterase) to investigate their impact of endogenous Crebrf expression. Figure 3-5 shows that treatment of murine adipocytes with adipogenesis stimulating hormones is not sufficient to increase Crebrf expression, but again demonstrating that increased levels of cAMP reduced Crebrf expression.

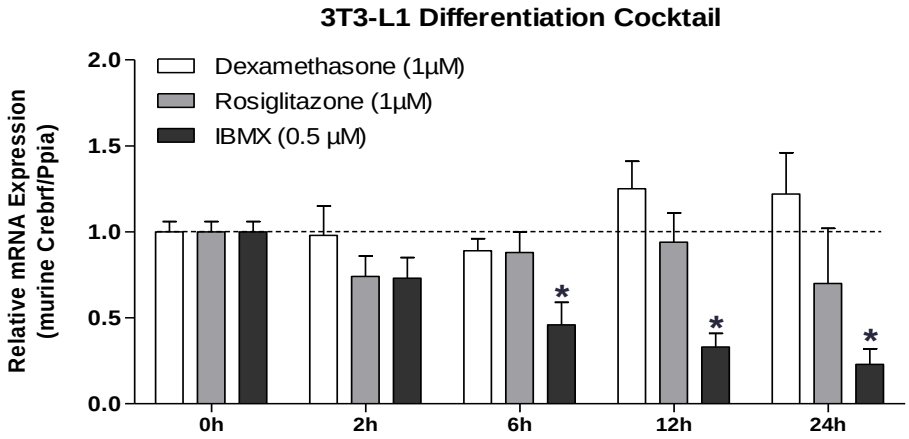

Figure 3-5: Endogenous expression of Crebrf in 3T3-L1 mature adipocytes cannot be further increased by treatment with adipogenesis stimulating hormones. Samples were generated on indicated time points and mRNA expression was measured using RT-qPCR. Relative mRNA expression of Crebrf is normalized to the housekeeping gene Cyclophilin (peptidylprolyl isomerase A; PPia). $p \leq .05$: * effect of treatment.

3.4 Crebrf expression is upregulated in adipogenesis of 3T3-L1 cells

Since *Minster et. al.* demonstrated that overexpression of CREBRF improves adipogenesis by increasing lipid storage and expression of adipogenesis marker in 3T3 adipocytes [24], we were wondering whether Crebrf expression itself was affected by adipocyte differentiation. Adipogenesis was induced in 3T3-L1 preadipocytes by treatment with a hormonal differentiation cocktail. To confirm adipocyte differentiation, we first visualized lipid accumulation by staining preadipocytes and adipocytes with Oil Red O dye, shown in Figure 3-6.

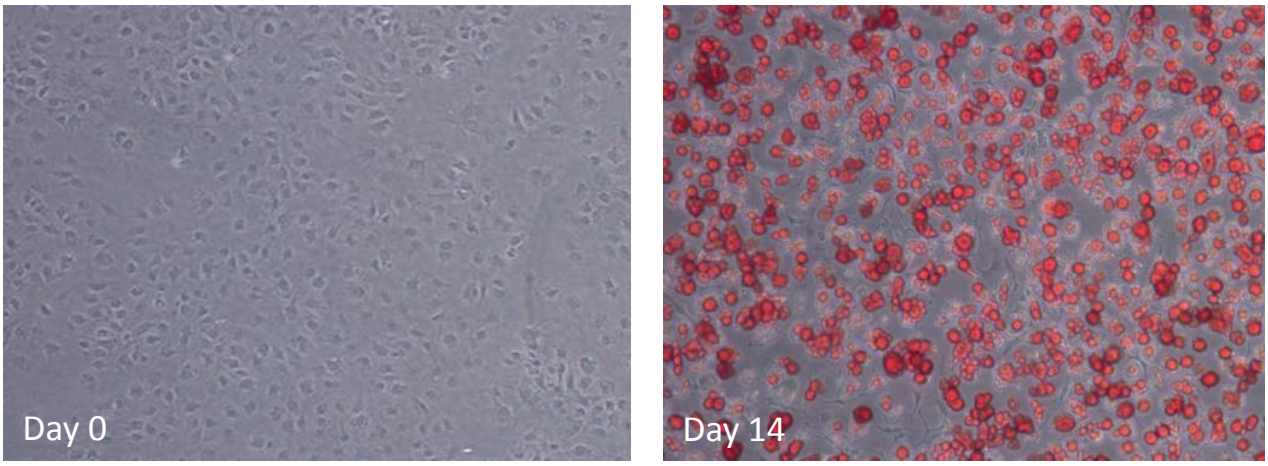

Figure 3-6: Oil Red O Staining of 3T3-L1 cells. Preadipocytes (day 0) and adipocytes (day 14) were stained with Oil Red O to visualize lipid accumulation here in red. 20x magnification.

Relative lipid accumulation in course of adipogenesis of 3T3-L1 cells was assessed by extracting Oil Red O dye from cells stained on several time points of the differentiation. The amount of incorporated dye for each time point is reflected by the absorption of Oil Red O dye at 512 nm (OD_{512}) and clearly showed increase lipid levels following differentiation (Figure 3-7).

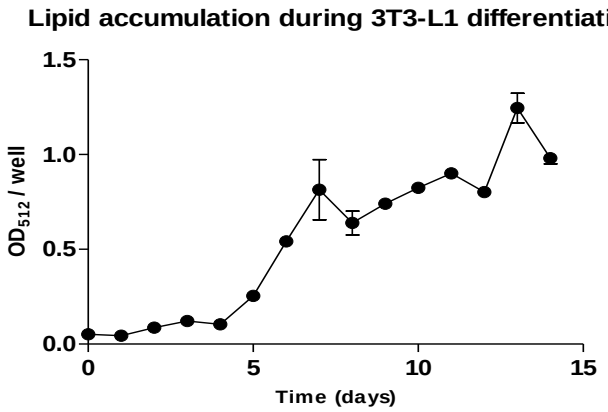

Figure 3-7: Accumulation of lipids during adipogenesis of 3T3-L1 cells, quantified with Oil Red O staining. 3T3-L1 cells were stained with Oil Red O dye on several time points. Dye was extracted from each well (n=3) and absorption at 512nm was measured using a spectrophotometry. The amount of incorporated dye reflects the lipid content in the cells.

To evaluate whether 3T3-L1 cells were fully differentiated to adipocytes, the mRNA expression of key adipogenic markers such as C/EBPα (expressed during late differentiation), PPARγ2 (expressed during early differentiation), and Adiponectin (expressed by mature adipocytes) was determined. As expected, the expression of these target genes increased during the differentiation process. Notably, Crebrf expression increased in the first days of differentiation (starting on day 1) and reaching its peak on day 5 – 6 of differentiation (Figure 3-8). These data showed that Crebrf expression is induced during adipocyte differentiation in murine adipocytes, suggesting that CREBRF might contribute to adipogenesis.

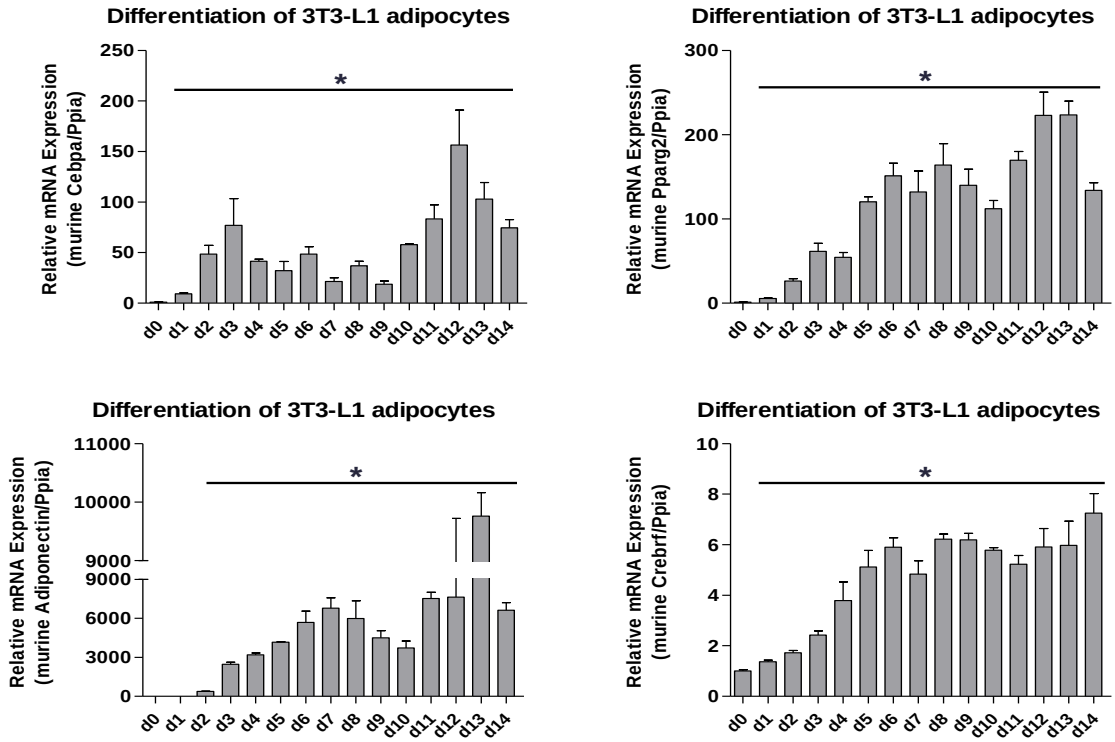

Figure 3-8: Endogenous expression of adipogenic markers and Crebrf in murine 3T3-L1 cells after induction of differentiation. Samples were generated on indicated time points and mRNA expression was measured using RT-qPCR. **a)** Relative mRNA expression of C/EBPα (Cebpa) normalized to the housekeeping gene Cyclophilin (peptidylprolyl isomerase A; PPia). **b)** Relative mRNA expression of PPARγ2 normalized to Cyclophilin. **c)** Relative mRNA expression of Adiponectin normalized to Cyclophilin. **d)** Relative mRNA expression of Crebrf normalized to Cyclophilin. $p \leq .05$: * effect of treatment.

3.5 Crebrf is expressed in various adipose tissue deposits, but its expression is not dependent on the diet

Since Crebrf expression is induced during the process of adipogenesis and promoting increased lipid accumulation, we evaluated whether Crebrf expression is changed in the presence of increased lipid levels. Therefore, we compared the expression of Crebrf in different adipose tissue deposits (BAT, brown, PGAT, perigonadal, and SCAT, subcutaneous adipose tissue) from 12 week old mice fed chow or high fat diet (HFD) (figure 3-9). Although, Crebrf is expressed in all adipose tissues, its expression is different between the deposits. Interestingly, HFD feeding had no effect on Crebrf expression in white adipose tissue, but was increased in brown adipose tissue.

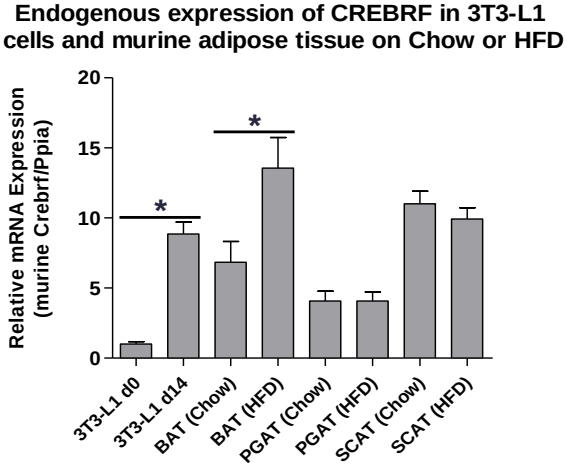

Figure 3-9: In vitro and in vivo expression of murine Crebrf. Relative mRNA expression of murine Crebrf normalized to the housekeeping gene Cyclophilin (peptidylprolyl isomerase A; PPia). 3T3-L1 preadipocytes were collected on day 0 of differentiation, 3T3-L1 adipocytes were collected on day 14 of differentiation. 12 week old control mice (C57/Bl6-N) were fed chow and high fat diet (HFD; mice were fed HFD for 8 weeks), fasted for 4h, adipose tissue was collected, RNA isolated, cDNA generated and relative mCrebrf expression relative to cyclophilin reference gene was determined by qPCR with 3T3-L1 preadipocytes arbitrarily set to 1. (BAT, brown; PGAT, perigonadal; SCAT, subcutaneous adipose tissue), n=3-10/group. $p \leq .05$: * effect of treatment.

3.6 Deletion of Crebrf in C57/Bl6-J mice increases total body fat mass

As already published in drosophila, adult REPTOR-knock out flies show reduced triglyceride levels, lower body weight, and increased sensitivity to starvation [27]. To investigate the contribution of CREBRF on lipid and energy metabolism in mice, C57/Bl6-J Crebrf-KO mice were generated. Validation of global Crebrf-KO in C57/Bl6-J mice demonstrated a drastic reduction of Crebrf expression in various tissues of 21 week old Crebrf-KO mice, (Figure 3-10a). Control and Crebrf-KO mice fed chow diet were weighed weekly. Longitudinal bodyweight showed a trend of increased bodyweight in Crebrf-KO mice compared to their control mice (Figure 3-10b).To determine body composition, fat and lean mass were assessed every 4 weeks using Echo-MRI (Figure 3-10c&d)Surprisingly, fat mass was significantly increased while lean mass was decreased in Crebrf-KO compared to control mice. Consistently, white adipose tissue mass

such as perigonadal (PGAT) and subcutaneous (SCAT) adipose tissue was increased in 21 week old Crebrf-KO mice. In contrast, brown adipose tissue was similar. Non-adipose tissue weight did not differ between Crebrf-KO and control mice (Figure 3-10e&f). Hence, these data suggest that deletion of CREBRF in mice increases total fat mass and therefore affects lipid metabolism differently compared to *drosophila melanogaster*.

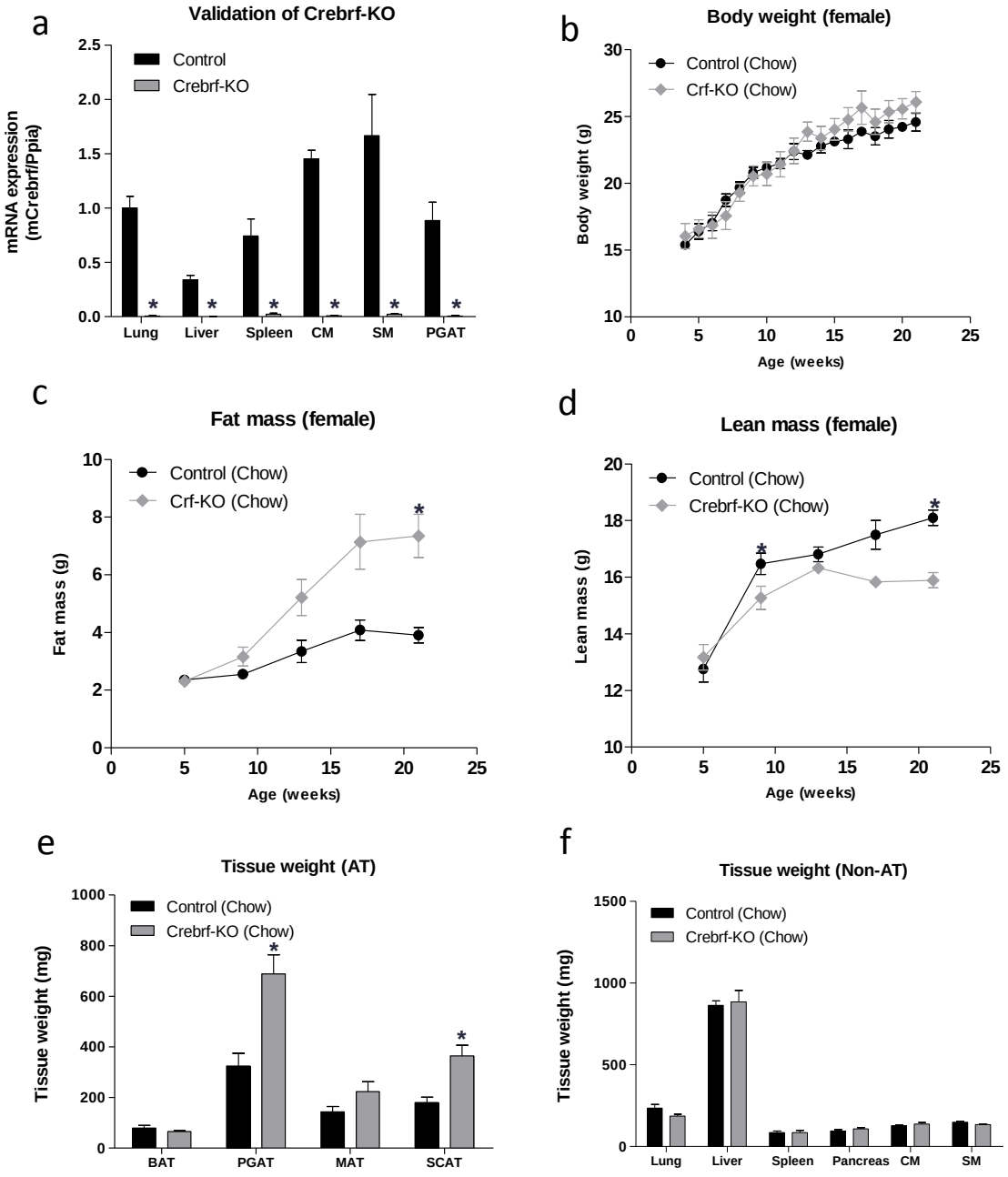

Figure 3-10: Validation of Crebrf-KO in C57/Bl6-J mice and comparison of bodyweight, fat mass, lean mass, and tissue weight between wildtype and knock out mice. a) 21 week old control and Crebrf-KO mice fed chow diet were fasted for 16h. Tissue was collected and relative mRNA expression of Crebrf was determined by qPCR with control lung arbitrarily set to 1. Cyclophilin was used as reference gene. (CM, cardiac muscle; SM, smooth muscle; PGAT, perigonadal adipose tissue), n=5-6/group. **b)** Longitudinal bodyweight of Control and Crebrf-KO mice on Chow diet. **c & d)** Longitudinal fat and lean mass by EchoMRI. **e & f)** Adipose and Non-Adipose tissue weight of 21 week old control and Crebrf-KO mice fed chow diet. $p \leq .05$: * effect of treatment.

3.7 Expression of adipogenic markers are not changed in Crebrf-KO

Although, Crebrf expression is increased during adipogenesis in our cell model, Crebrf-KO mice showed not the expected reduction in fat mass, but instead had increased WAT mass. To investigate whether the loss of Crebrf affects adipogenesis or lipogenesis, the expression of adipogenic and lipogenic markers in the brown (BAT), perigonadal (PGAT) and subcutaneous adipose tissue (SCAT) was assessed in 21 week old control and Crebrf-KO mice fed chow diet. Notably, there were no fundamental differences found between Crebrf-KO and control mice shown in Figure 3-11, indicating that the loss of Crebrf does not alter adipogenesis or that other transcription factors might replace the transcriptional function of Crebrf.

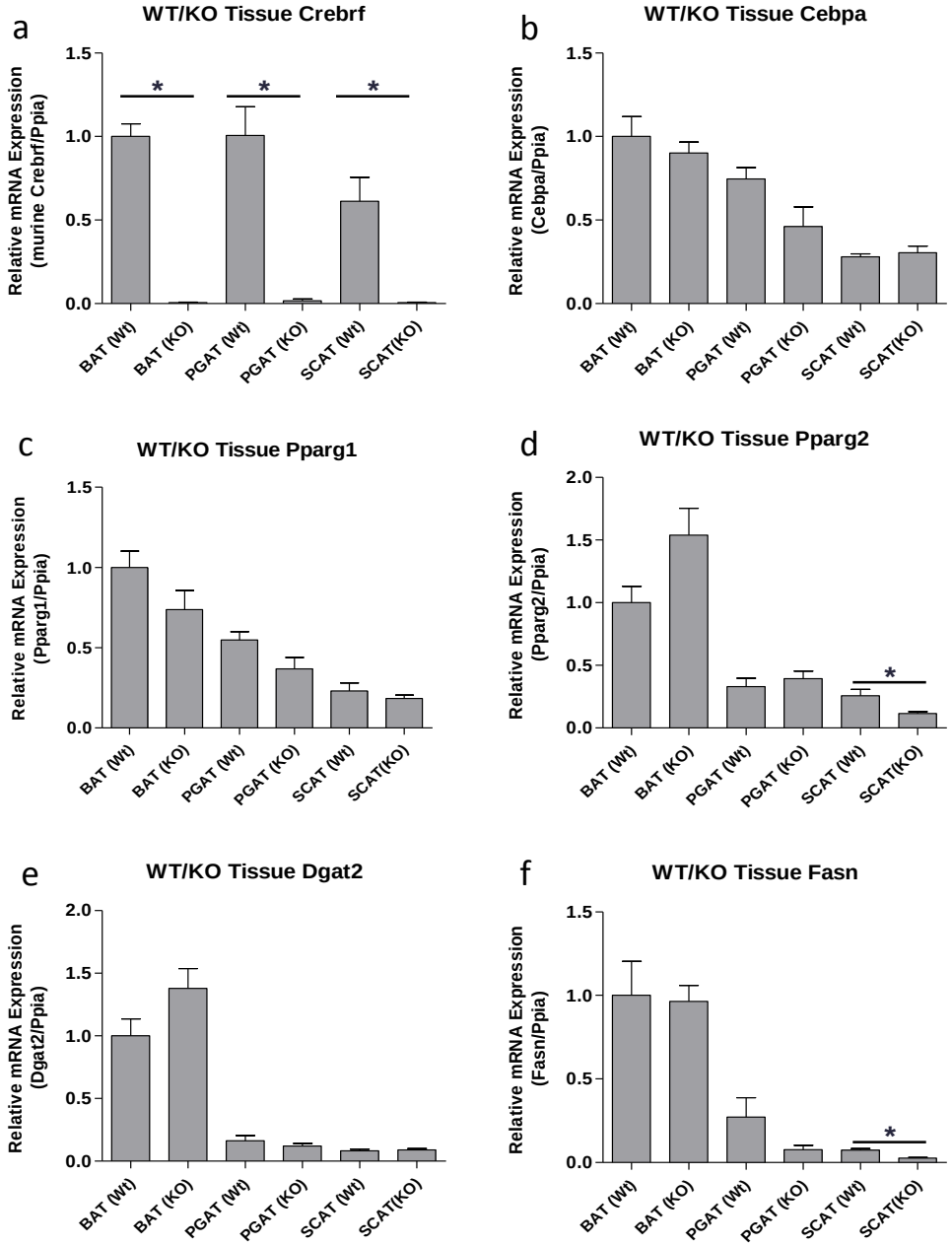

Figure 3-11: Expression of adipogenic and lipogenic markers in Crebrf-KO and control mice. 21 week old control and Crebrf-KO mice fed chow diet were fasted for 16h. Adipose tissue was collected and relative mRNA expression of a) Crebrf, b-d) adipogenic markers PPARγ 1/2 and of C/EBPα, and e, f) lipogenic markers Dgat2 and Fasn were determined by qPCR with control BAT arbitrarily set to 1. Cyclophilin was used as reference gene. (BAT, brown adipose tissue; PGAT, perigonadal adipose tissue; SCAT, subcutaneous adipose tissue; Dgat2, diacylglycerol O-acyltransferase 2; Fasn, Fatty acid synthase), n=5-6/group. $p \leq .05$: * effect of treatment.

3.8 Nutritional stress regulates endogenous *CREBRF* expression in human adipocytes

To evaluate whether human *CREBRF* is also regulated by nutritional stress, we measured endogenous *CREBRF* expression in HPAC adipocytes. Cells were treated again with HBSS (with glucose, but no amino acids), serum-free DMEM (with glucose and amino acids, but no FA) or complete DMEM containing 20 ng/mL Rapamycin. Starving and Rapamycin treatment of HPAC adipocytes induced CREBRF expression (Figure 3-12). Re-feeding of starved cells abrogates this effect. Thus, induction of CREBRF expression under nutritional stress is conserved from fly to mammalians including mice and humans.

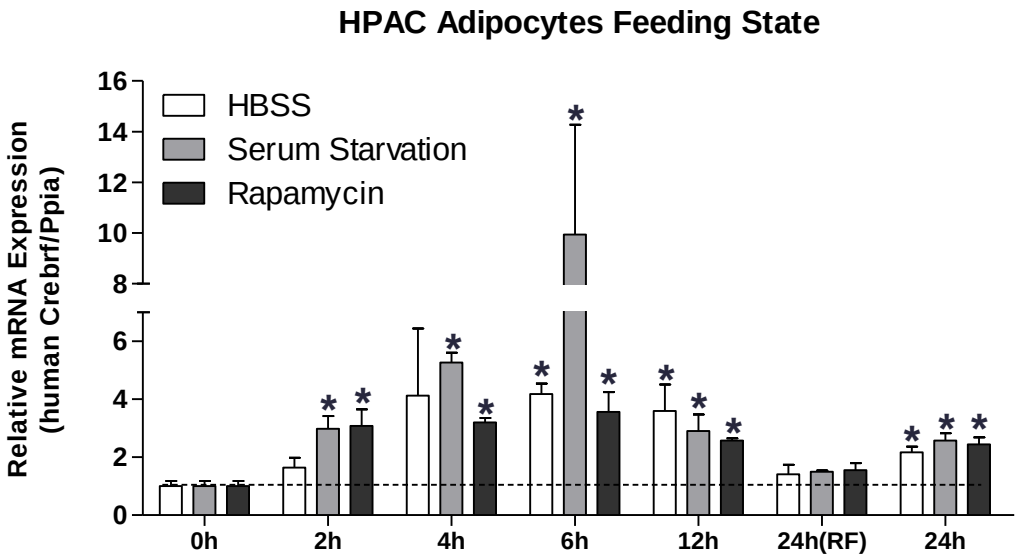

Figure 3-12: Endogenous expression of *CREBRF* in human adipocytes in response to nutritional status. Expression was measured using RT-qPCR on indicated time points after induction of nutritional stress (t=0h). The abbreviation RF indicates that cells were re-fed with complete medium after 12 h. Relative mRNA expression of *CREBRF* normalized to the housekeeping gene Cyclophilin (peptidylprolyl isomerase A; PPia) in adipocytes (day 21 of differentiation) with t=0h group arbitrarily set to 1. $p \leq .05$: * effect of treatment.

3.9 *CREBRF* expression is upregulated during adipogenesis in human adipocytes

Since murine Crebrf expression increased during adipocyte differentiation, we evaluated whether human *CREBRF* showed a similar expression pattern following adipogenesis. We treated HPACs with a hormonal differentiation cocktail to initiate adipogenesis. Adipocyte differentiation was observed by increased accumulation of lipid in HPAC cells (Figure 3-13 and figure 3-14).

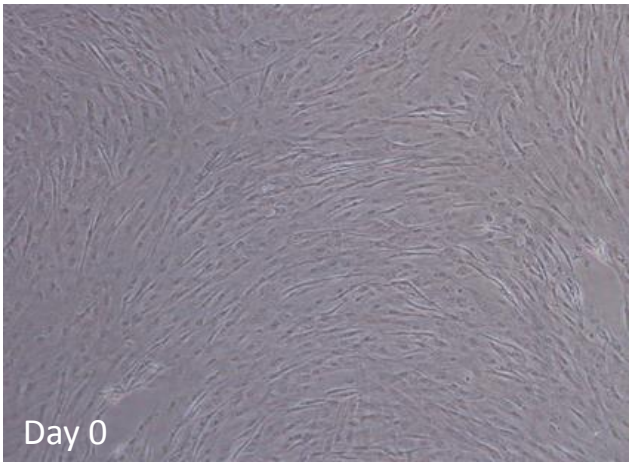

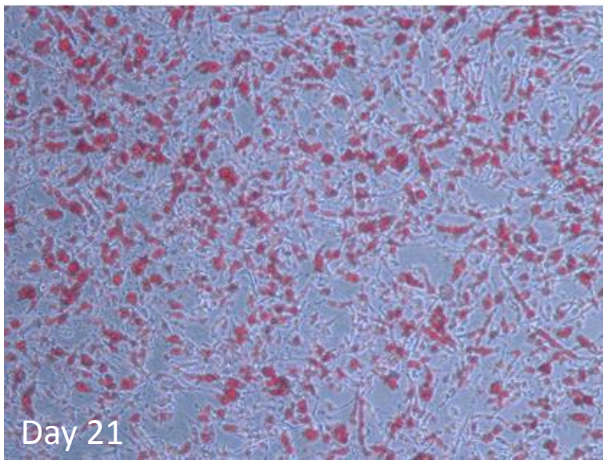

Figure 3-13: Oil Red O Staining of HPAC cells. Preadipocytes (day 0) and adipocytes (day 21) were stained with Oil Red O to visualize lipid accumulation. 20x magnification.

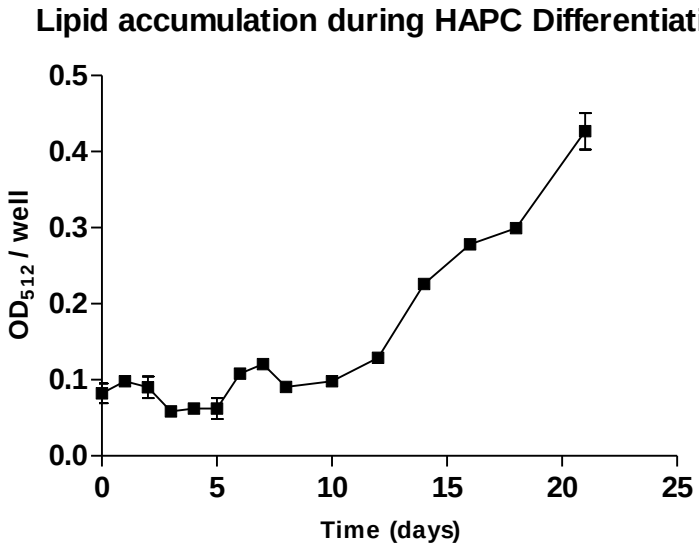

Figure 3-14: Accumulation of lipids during adipogenesis of HPACs, quantified with Oil Red O staining. HPAC cells were stained with Oil Red O dye on several time points. Dye was extracted from each well (n=3) and absorption at 512nm was measured using spectrophotometry. The amount of incorporated dye reflects the lipid content of the cells.

Likewise, the expression of adipogenic markers such as PPPARγ2 and CEBPβ (two markers for early adipogenesis) was elevated during adipocyte differentiation (figure 3-15) confirming a sufficient differentiation. HPAC adipocytes gad higher mRNA levels of CREBRF compared to human preadipocytes (figure 3-16), demonstrating that CREBRF expression is also upregulated during adipogenesis in human adipocytes.

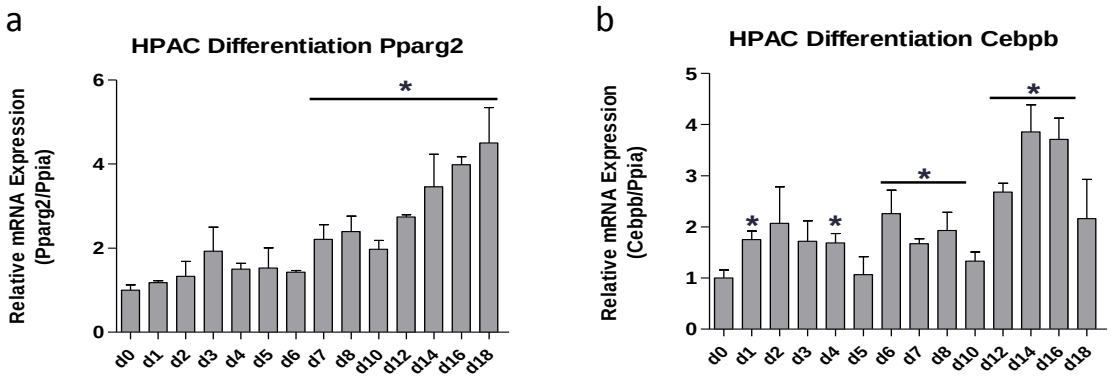

Figure 3-15: Endogenous expression of adipogenic markers in HPAC cells after induction of differentiation. Samples were generated on indicated time points and mRNA expression was measured using RT-qPCR. **a)** Relative mRNA expression of PPARγ2 normalized to the housekeeping gene Cyclophilin (peptidylprolyl isomerase A; PPia). **b)** Relative mRNA expression of C/EBPβ (Cebpb) normalized to Cyclophilin. $p \leq .05$: * effect of treatment.

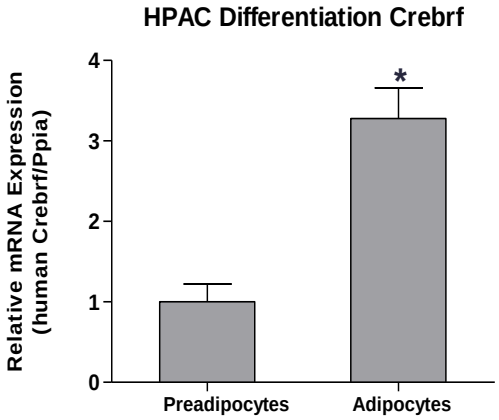

Figure 3-16: Endogenous expression of CREBRF in human HPAC cells after induction of differentiation. Relative mRNA expression of *CREBRF* in preadipocytes (day 0) and adipocytes (day 21 of differentiation) normalized to the housekeeping gene Cyclophilin (peptidylprolyl isomerase A; PPia). $p \leq .05$: * effect of treatment.

3.10 Chronic overexpression of CREBRF in SGBS cells using lentivirus

Since previous studies showed that overexpression of human CREBRF in murine adipocytes alters cellular bioenergetics [24], we wondered whether this is also true for human adipocytes. We evaluated the contribution of CREBRF-WT and CREBRF-RQ, the obesity-risk variant, to metabolic outcome such as mitochondrial respiration in human adipocytes. We generated lentiviruses to overexpress human CREBRF-WT and CREBRF-RQ. Therefore, we cloned CREBRF-WT and CREBRF-RQ in pLVX-Tight-Puro Vector (Figure 3-17).

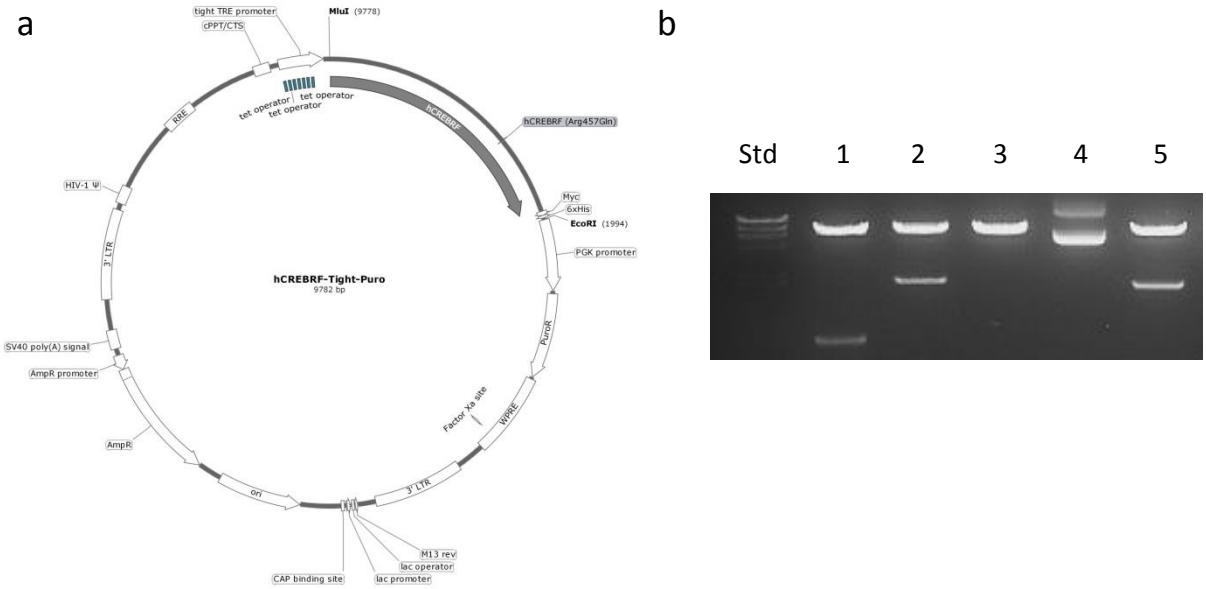

Figure 3-17: Generation of hCREBRF lentiviruses: a) Vector map of Tight-Puro containing CREBRF-WT or CREBRF-RQ. Tight-Puro vector has a TRE promoter and encodes for C-terminal Myc-6x(His) tag. Additionally, the expression vector contains an ampicillin and neomycin. **b)** Agarose gel picture. DNA Standard Lambda DNA/HindIII Marker (Thermo Scientific™) was used as a standard. 1) GFP-Tight Puro, cut with EcoRI and MluI; 2) human Crebrf-RQ-Tight Puro, cut with EcoRI and MluI; 3) Tight-Puro, cut with EcoRI; 4) uncut Tight-Puro; 5) human Crebrf-WT-Tight Puro, cut with BamHI/EcoRI.

Positive pLVX-Tight-Puro-CREBRF constructs and the pLVX-Tet-Off Advanced Vector were used to transfect HEK-293T cells to generate lentiviruses. Afterwards, SBGS cells were co-transducted with lentiviral supernatants overexpressing CREBRF-WT or CREBRF-RQ and Tet-Off and were subjected to selective pressure using Puromycin to isolate and amplify only CREBRF overexpressing SGBS cells.

3.11 Measuring mitochondrial function of in SGBS preadipocytes

Previous studies showed that overexpression of CREBRF-WT and CREBRF-RQ differently regulates mitochondrial respiration in murine adipocytes [24]. To verify whether CREBRF overexpression also affects mitochondrial function in the preadipocyte state, we used SGBS preadipocytes stably overexpressing CREBRF for Seahorse measurement. We determined oxygen consumption rate (OCR) over time (Figure 3-18a). We measured ATP production (after addition of Oligomycin) (Figure 3-18b), basal cellular respiration (Figure 3-18c) as well as maximal respiration (after addition of FCCP) (Figure 3-18d). Both, overexpression of CREBRF-WT and CREBRF-RQ increased mitochondrial function compared to control cells. However, the increase in OCR was much more pronounced in cells overexpressing the CREBRF-RQ variant. Likewise, basal glycolysis was increased in cells overexpressing CREBRF-WT, and again CREBRF-RQ overexpression drastically increased glycolysis rate (Figure 3-19) compared to CREBRF-WT.

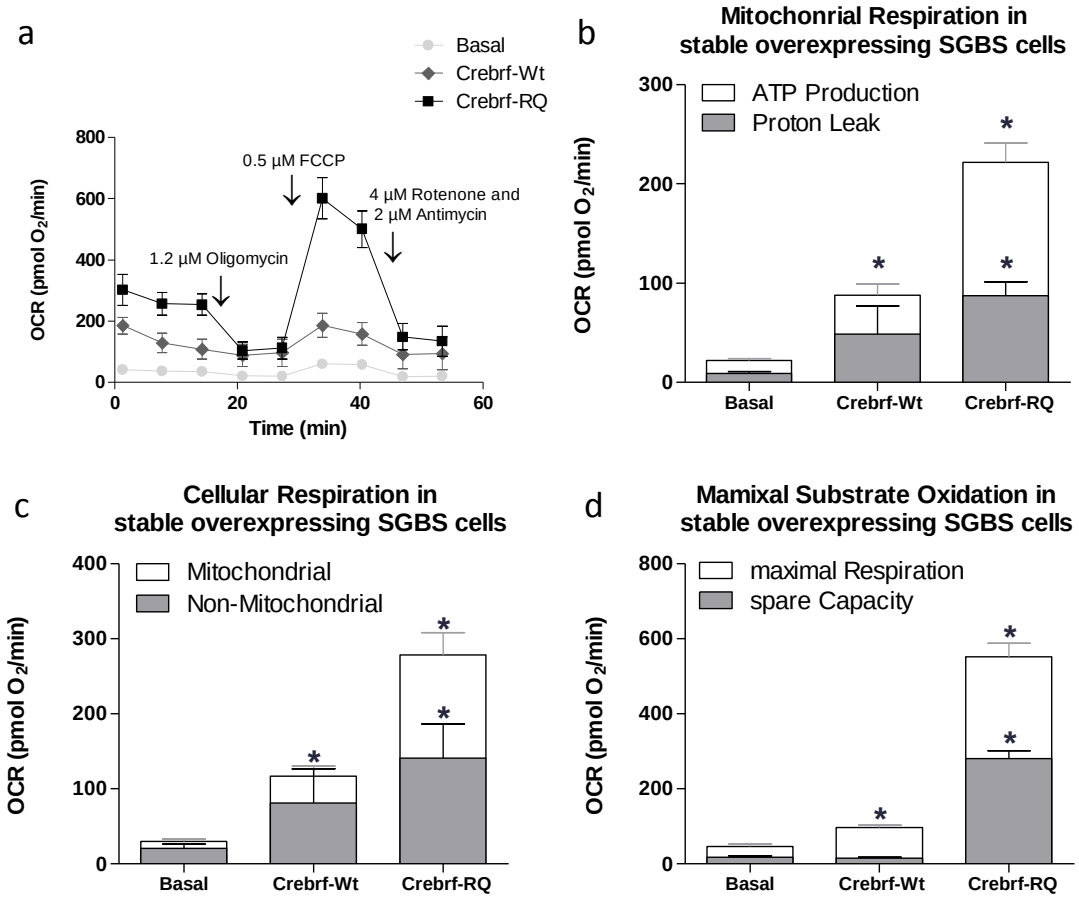

Figure 3-18: Mitochondrial respiration in SGBS preadipocytes overexpressing hCREBRF. a) Oxygen consumption rate (OCR) over time in SGBS preadipocytes. Mitochondrial Respiration was measured under basal conditions or after the addition of Oligomycin (1.2 µM; t=14.3 min) the chemical uncoupler FCCP (0.5 µM; t=27.3 min) or Antimycin/Rotenone (2 µM/4µM; t= 40.4 min). (n=6 wells/group). **b)** Mitochondrial respiration was dissected into ATP production and proton leak. **c)** Cellular respiration was dissected into mitochondrial and non-mitochondrial. **d)** Maximal respiration was dissected in spare capacity and maximal respiration. p ≤.05: * effect of treatment.

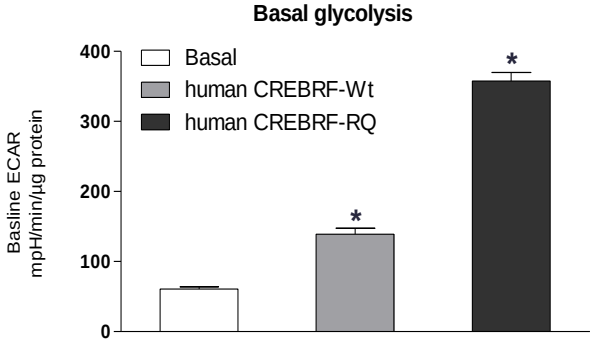

Figure 3-19: Glycolysis in SGBS preadipocytes overexpressing hCREBRF. Basal extracellular acidification rate (ECAR) was determined in SGBS preadipocytes. *p* ≤.05: * effect of treatment.

Overall, these data indicated that CREBRF directly affects mitochondrial respiration and glycolysis. These results are in contrast to previous published data [24], demonstrating that CREBRF-WT increases but CREBRF-RQ decreases mitochondrial function. The different observations might be caused by the fact that our data were obtained from human preadipocytes and the published data from murine adipocytes, suggesting that the mitochondrial ability differs between pre- and adipocyte state. Accordingly, Seahorse measurements in SGBS preadipocytes and adipocytes clearly demonstrated an increase in mitochondrial respiration following adipocyte differentiation (day 0 – day 7 – day 14) (Figures 3-20). Notably, mitochondrial respiration of SGBS preadipocytes overexpressing CREBRF was comparable to SGBS adipocytes on day 7 and day 14 of differentiation, suggesting that the presence of CREBRF promotes mitochondrial function.

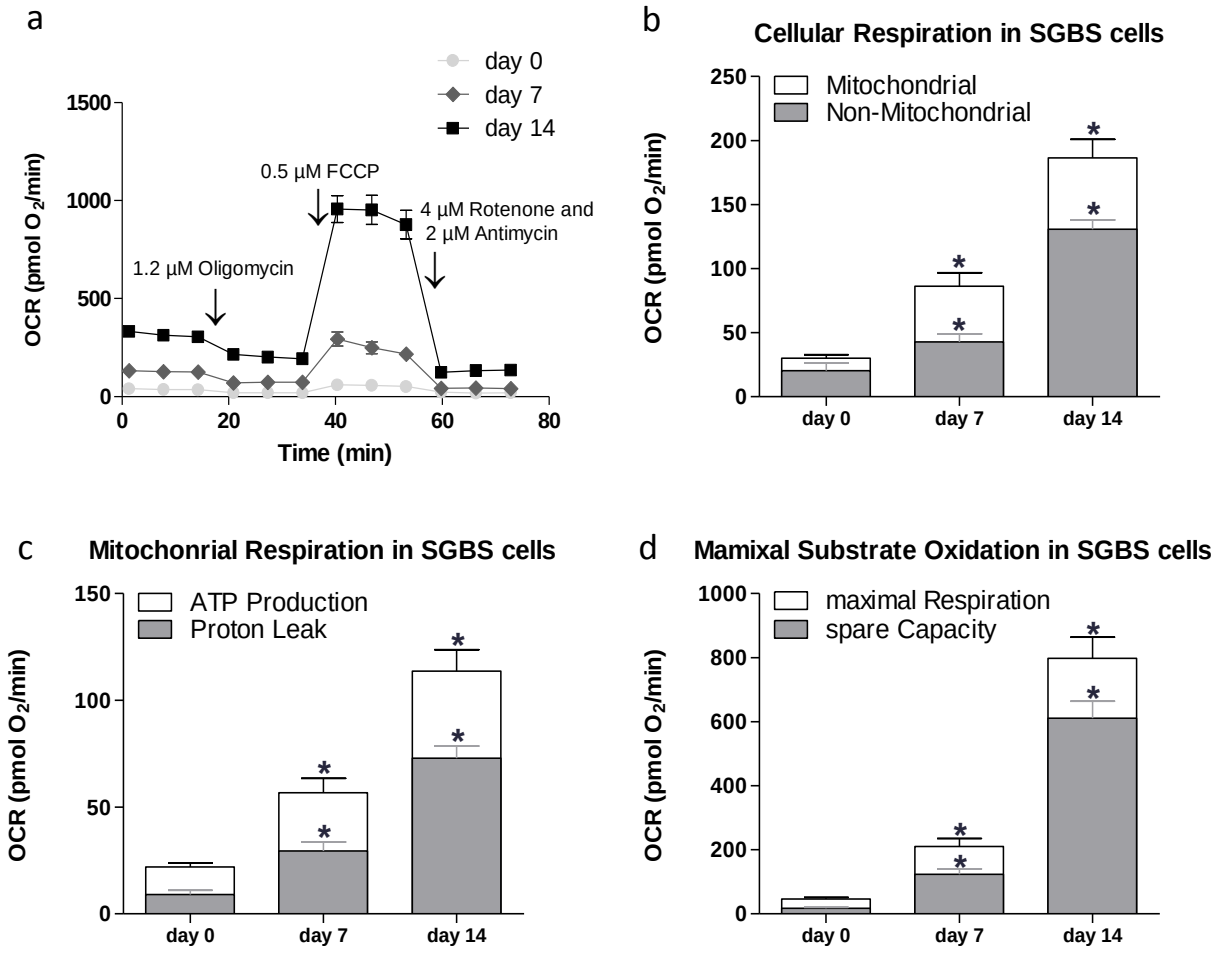

Figure 3-20: Mitochondrial respiration in SGBS during adipocyte differentiation. a) Oxygen consumption rate (OCR) over time in SGBS preadipocytes (day 0) and in adipocytes (day 7 and day 14 of differentiation). Mitochondrial Respiration was measured under basal conditions or after the addition of Oligomycin (1.2 µM; t=14.3 min) the chemical uncoupler FCCP (0.5 µM; t=33.8 min) or Antimycin/Rotenone (2 µM/4µM; t= 53.4 min). (n=6 wells/group). **b)** Cellular respiration was dissected into mitochondrial and non-mitochondrial. **c)** Mitochondrial respiration was dissected into ATP production and proton leak. **d)** Maximal respiration was dissected in spare capacity and maximal respiration. $p \leq .05$: * effect of treatment.

4. Conclusion and Discussion

In this study, we investigated the regulation of CREBRF in murine and human adipocytes and determined the contribution of overexpressing CREBRF and its obesity-risk variant to adipocyte function. We assessed the impact of CREBRF on adipocyte function on cellular levels using murine and human adipocytes and in a mouse model lacking Crebrf (Crebrf-KO). We found that 1) murine and human Crebrf is directly regulated by mTORC1. 2) Crebrf is upregulated during differentiation, but its absence does not change adipogenesis in various adipose tissue depots. 3) Deletion of Crebrf in mice results in increased total fat mass while 4) overexpression of CREBRF-WT and its obesity-risk variant promotes energy substrate use shown by increased mitochondrial respiration and glycolysis in human adipocytes.

Cell culture experiments performed in course of this study showed that Crebrf expression is regulated by nutritional status such as fasting, in a similar way as previously shown in *Drosophila melanogaster* [27]. Starvation changes cellular metabolism pathways like β-oxidation and lipolysis in order to achieve nutritional homeostasis [29]. Inhibition of mTORC1, by fasting or rapamycin treatment induced endogenous Crebrf expression, both in murine and human adipocyte cells. The opposite effect, decreased Crebrf mRNA expression in murine cells, was achieved by insulin treatment which prevents mTORC1 inhibition. These data indicate that endogenous Crebrf expression levels are directly regulated by mTORC1 activity.

Interestingly, murine Crebrf mRNA levels are decreased in response to elevated cAMP levels caused by activation of β-adrenergic receptors. Thus, stimulation of lipolysis via Isoproterenol, Forskolin, or CL treatment reduced Crebrf expression. These contradictive results demonstrating that stimulation of lipolysis decreases Crebrf expression, but starvation (which also promotes lipolysis) increases Crebrf expression suggest, that the upregulation of Crebrf in starved cells might rather be a response to elevated mitochondrial function (i.e. β-oxidation) than to changes in lipid metabolism.

Since it was previously shown that Crebrf overexpression promotes lipid accumulation in murine adipocytes [24], we were interested whether endogenous Crebrf levels are regulated during adipogenesis. Crebrf expression is increasing during the first days after inducing adipogenesis in murine cells, but its expression does not significantly change afterwards in mature adipocytes, when observed for prolonged time, indicating that Crebrf might play a role in the early phase of differentiation. However, deletion of Crebrf caused no fundamental changes in the expression of key adipogenic markers, suggesting that Crebrf is not crucial for the regulation of adipogenesis. Furthermore, the initial upregulation of Crebrf in the course of adipocyte differentiation might be caused by changes in cell morphology and the adaption to novel cellular functions such as induced mitochondrial biogenesis rather than the process of adipogenesis and lipid accumulation themselves.

This conclusion is also corroborated by the analyses of Crebrf-expression in adipose tissue of mice fed HFD. Although mice fed HFD have promoted lipid storage and increased fat mass, the endogenous Crebrf

expression in the white adipose tissue (WAT) did not differ from mice on control Chow diet. There was, however, a significant increase of endogenous Crebrf expression in the brown adipose tissue (BAT) of HFD fed mice. This finding might be due to the distinct functions and morphology of WAT and BAT. BAT is known to have significantly higher mitochondrial density, which allows for enhanced substrate oxidation and heat production [8].

Since studies in *Drosophila melanogaster* showed that the KO of the Crebrf-Orthologue Reptor results in lower triglyceride storage and body weight [27], we expected to see a similar phenotype in Crebrf-KO mice. Surprisingly, there was a trend of increased bodyweight in Crebrf-KO mice seen in longitudinal weight measurements. Also, the Crebrf-KO resulted in promoted lipid accumulation (fat mass) and increased WAT-weight (perigonadal and subcutaneous adipose tissue). This might be due to alterations in the energy substrate utilization such as lipid.

Accordingly, overexpression of CREBRF in human preadipocytes resulted in increased mitochondrial ATP production, basal mitochondrial and non-mitochondrial respiration as well as basal glycolysis, suggesting that CREBRF directly affects mitochondrial function. Spare respiratory capacity, which is considered as an indicator of how close cells operate to their bioenergetics limit [30], was drastically increased in Crebrf-RQ overexpressing preadipocytes. Whereas Crebrf-WT overexpressing and control preadipocytes showed rather low spare respiratory capacities, indicating that these cells only have a modest ability to adapt to increased energy demands of cells. Notably, oxygen consumption rates (OCRs) of human preadipocytes overexpressing Crebrf-RQ closely resemble OCRs of mature adipocytes [31].

Interestingly and unexpected to recently published data [24], we were not able to detect energy-saving properties of Crebrf-RQ overexpression in mitochondrial function of human preadipocytes, as previously observed in murine adipocytes. These data indicate that the impact of CREBRF-RQ on mitochondrial respiration might be dependent on the availability of mitochondria in cells. Consistently, we demonstrated that in the state of preadipocytes mitochondrial respiration is low while adipocytes differentiation promotes mitochondrial respiration due to increases mitochondrial biogenesis [32]. Therefore, the differences in our study might be caused by the use of preadipocytes instead of adipocytes. In the near future we will determine mitochondrial respiration in adipocytes overexpressing CREBRF.

5. Acknowledgement

First and foremost, I would like to thank the Austrian Marshall Plan Foundation which has funded my research fellowship at the Division of Endocrinology and Metabolism at the University of Pittsburgh. The Austrian Marshall Plan Foundation Scholarship gave me the chance to conduct research for my Master's thesis in the United States of America.

Furthermore I would like to thank Dr. Erin Kershaw, for the opportunity to join her research group and her support throughout my research fellowship.

I would like to give special thanks to Dr. Gabriele Schoiswohl, for her invaluable support and excellent supervision of this thesis. She impressed me with her outstanding theoretical and practical knowledge and I am grateful for her thoughtful advices.

Also, I would like to thank Laura, who was always helpful and made the time at the University of Pittsburgh unforgettable.

6. References

1 WHO. *Obesity and overweight Fact Sheet*, <http://www.who.int/mediacentre/factsheets/fs311/en/> (June 2016).

2 Kopelman, P. G. Obesity as a medical problem. *Nature* **404**, 635-643, doi:10.1038/35007508 (2000).

3 Ouchi, N., Parker, J. L., Lugus, J. J. & Walsh, K. Adipokines in inflammation and metabolic disease. *Nat Rev Immunol* **11**, 85-97, doi:10.1038/nri2921 (2011).

4 Peirce, V., Carobbio, S. & Vidal-Puig, A. The different shades of fat. *Nature* **510**, 76-83, doi:10.1038/nature13477 (2014).

5 Wronska, A. & Kmiec, Z. Structural and biochemical characteristics of various white adipose tissue depots. *Acta Physiol (Oxf)* **205**, 194-208, doi:10.1111/j.1748-1716.2012.02409.x (2012).

6 Tilg, H. & Moschen, A. R. Adipocytokines: mediators linking adipose tissue, inflammation and immunity. *Nat Rev Immunol* **6**, 772-783, doi:10.1038/nri1937 (2006).

7 Mathieu, P., Poirier, P., Pibarot, P., Lemieux, I. & Després, J. P. Visceral obesity: the link among inflammation, hypertension, and cardiovascular disease. *Hypertension* **53**, 577-584, doi:10.1161/HYPERTENSIONAHA.108.110320 (2009).

8 Oelkrug, R., Polymeropoulos, E. T. & Jastroch, M. Brown adipose tissue: physiological function and evolutionary significance. *J Comp Physiol B* **185**, 587-606, doi:10.1007/s00360-015-0907-7 (2015).

9 Nedergaard, J., Bengtsson, T. & Cannon, B. Three years with adult human brown adipose tissue. *Ann N Y Acad Sci* **1212**, E20-36, doi:10.1111/j.1749-6632.2010.05905.x (2010).

10 Spalding, K. L. *et al.* Dynamics of fat cell turnover in humans. *Nature* **453**, 783-787, doi:10.1038/nature06902 (2008).

11 Rigamonti, A., Brennand, K., Lau, F. & Cowan, C. A. Rapid cellular turnover in adipose tissue. *PLoS One* **6**, e17637, doi:10.1371/journal.pone.0017637 (2011).

12 Gesta, S., Tseng, Y. H. & Kahn, C. R. Developmental origin of fat: tracking obesity to its source. *Cell* **131**, 242-256, doi:10.1016/j.cell.2007.10.004 (2007).

13 Cristancho, A. G. & Lazar, M. A. Forming functional fat: a growing understanding of adipocyte differentiation. *Nat Rev Mol Cell Biol* **12**, 722-734, doi:10.1038/nrm3198 (2011).

14 Moseti, D., Regassa, A. & Kim, W. K. Molecular Regulation of Adipogenesis and Potential Anti-Adipogenic Bioactive Molecules. *Int J Mol Sci* **17**, doi:10.3390/ijms17010124 (2016).

15 Tang, Q. Q., Otto, T. C. & Lane, M. D. Mitotic clonal expansion: a synchronous process required for adipogenesis. *Proc Natl Acad Sci U S A* **100**, 44-49, doi:10.1073/pnas.0137044100 (2003).

16 Ravnskjaer, K., Madiraju, A. & Montminy, M. Role of the cAMP Pathway in Glucose and Lipid Metabolism. *Handb Exp Pharmacol* **233**, 29-49, doi:10.1007/164_2015_32 (2016).

17 Lefterova, M. I. & Lazar, M. A. New developments in adipogenesis. *Trends Endocrinol Metab* **20**, 107-114, doi:10.1016/j.tem.2008.11.005 (2009).

18 Luo, L. & Liu, M. Adipose tissue in control of metabolism. *J Endocrinol* **231**, R77-R99, doi:10.1530/JOE-16-0211 (2016).

19 Cao, G. *et al.* Molecular cloning and characterization of a novel human cAMP response element-binding (CREB) gene (CREB4). *J Hum Genet* **47**, 373-376, doi:10.1007/s100380200053 (2002).

20 Raggo, C. *et al.* Luman, the cellular counterpart of herpes simplex virus VP16, is processed by regulated intramembrane proteolysis. *Mol Cell Biol* **22**, 5639-5649 (2002).

21 DenBoer, L. M. *et al.* Luman is capable of binding and activating transcription from the unfolded protein response element. *Biochem Biophys Res Commun* **331**, 113-119, doi:10.1016/j.bbrc.2005.03.141 (2005).
22 Liang, G. *et al.* Luman/CREB3 induces transcription of the endoplasmic reticulum (ER) stress response protein Herp through an ER stress response element. *Mol Cell Biol* **26**, 7999-8010, doi:10.1128/MCB.01046-06 (2006).
23 Audas, T. E., Li, Y., Liang, G. & Lu, R. A novel protein, Luman/CREB3 recruitment factor, inhibits Luman activation of the unfolded protein response. *Mol Cell Biol* **28**, 3952-3966, doi:10.1128/MCB.01439-07 (2008).
24 Minster, R. L. *et al.* A thrifty variant in CREBRF strongly influences body mass index in Samoans. *Nat Genet* **48**, 1049-1054, doi:10.1038/ng.3620 (2016).
25 Fischer-Posovszky, P., Newell, F. S., Wabitsch, M. & Tornqvist, H. E. Human SGBS cells - a unique tool for studies of human fat cell biology. *Obes Facts* **1**, 184-189, doi:10.1159/000145784 (2008).
26 Martyn, A. C. *et al.* Luman/CREB3 recruitment factor regulates glucocorticoid receptor activity and is essential for prolactin-mediated maternal instinct. *Mol Cell Biol* **32**, 5140-5150, doi:10.1128/MCB.01142-12 (2012).
27 Tiebe, M. *et al.* REPTOR and REPTOR-BP Regulate Organismal Metabolism and Transcription Downstream of TORC1. *Dev Cell* **33**, 272-284, doi:10.1016/j.devcel.2015.03.013 (2015).
28 Saxton, R. A. & Sabatini, D. M. mTOR Signaling in Growth, Metabolism, and Disease. *Cell* **168**, 960-976, doi:10.1016/j.cell.2017.02.004 (2017).
29 Turner, N., Cooney, G. J., Kraegen, E. W. & Bruce, C. R. Fatty acid metabolism, energy expenditure and insulin resistance in muscle. *J Endocrinol* **220**, T61-79, doi:10.1530/JOE-13-0397 (2014).
30 Brand, M. D. & Nicholls, D. G. Assessing mitochondrial dysfunction in cells. *Biochem J* **435**, 297-312, doi:10.1042/BJ20110162 (2011).
31 Keuper, M. *et al.* Spare mitochondrial respiratory capacity permits human adipocytes to maintain ATP homeostasis under hypoglycemic conditions. *FASEB J* **28**, 761-770, doi:10.1096/fj.13-238725 (2014).
32 Cedikova, M. *et al.* Mitochondria in White, Brown, and Beige Adipocytes. *Stem Cells Int* **2016**, 6067349, doi:10.1155/2016/6067349 (2016).